Transportation Research Part B 122 (2019) 436–456

Contents lists available at ScienceDirect

Transportation Research Part B

journal homepage: www.elsevier.com/locate/trb

The electric autonomous dial-a-ride problem

Claudia Bongiovanni[a], Mor Kaspi[a,b], Nikolas Geroliminis[a,*]

[a] Urban Transport Systems Laboratory, School of Architecture, Civil and Environmental Engineering, École Polytechnique Fédérale de Lausanne (EPFL), Lausanne CH-1015, Switzerland
[b] Department of Industrial Engineering, Tel-Aviv University, Tel-Aviv 69978, Israel

ARTICLE INFO

Article history:
Received 25 October 2017
Revised 17 February 2019
Accepted 1 March 2019
Available online 16 March 2019

Keywords:
Dial-a-Ride problem
Branch-and-cut
Electric autonomous vehicles

ABSTRACT

In the Dial-a-Ride-Problem (DARP) a fleet of vehicles provides shared-ride services to users specifying their origin, destination, and preferred arrival time. Typically, the problem consists of finding minimum cost routes, satisfying operational constraints such as time-windows, origin-destination precedences, user maximum ride-times, and vehicle maximum route-durations. This paper presents a problem variant for the DARP which considers the use of electric autonomous vehicles (e-ADARP). The problem covers battery management, detours to charging stations, recharge times, and selection of destination depots, along with classic DARP features. The goal of the problem is to minimize a weighted objective function consisting of the total travel time of all vehicles and excess ride-time of the users. We formulate the problem as a 3-index and a 2-index mixed-integer-linear program and devise a branch-and-cut algorithm with new valid inequalities derived from e-ADARP properties. Computational experiments are performed on adapted benchmark instances from DARP literature and on instances based on real data from Uber Technologies Inc. Instances with up to 5 vehicles and 40 requests are solved to optimality.

1. Introduction

The Dial-a-Ride Problem (DARP) is a class of combinatorial optimization problems which arises in the context of on-demand transportation systems. In its standard version, the problem consists of defining minimum cost routes and schedules for a fleet of vehicles exiting a common depot and serving a set of customers with given pickup and dropoff locations, as well as corresponding pickup or dropoff times. Static versions of the DARP assume all transportation requests are known in advance and need to be satisfied. After serving all customers, and by the end of the driver shifts, the vehicles are required to return to a common destination depot. Typical operational limitations include capacity, duration, time-window, and ride-time constraints (Cordeau and Laporte, 2003).

The DARP is a generalization of well-known optimization problems, such as the Traveling Salesman Problem (TSP), the Vehicle Routing Problem (VRP), and can also be viewed as a special case of the Pickup and Delivery Problem (PDP) (Toth and Vigo, 2014). As noted in (Cordeau and Laporte, 2003), the DARP is more challenging than other routing problems due to the need to weight transportation cost and user inconvenience against each other. A single operational objective does not provide an incentive to optimize service quality. As such, several DARP variants have considered a combination of operational and quality-related objectives (see Section 3.3.2 in Molenbruch et al. (2017a)). In fact, considering a fixed feasible routing

* Corresponding author.
E-mail addresses: claudia.bongiovanni@epfl.ch (C. Bongiovanni), morkaspi@tauex.tau.ac.il (M. Kaspi), nikolas.geroliminis@epfl.ch (N. Geroliminis).

https://doi.org/10.1016/j.trb.2019.03.004
0191-2615/

solution, the quality of service may be improved by minimizing a quality-oriented objective at no additional operational cost (Parragh, 2011). In this paper, the cost is defined by means of a weighted objective function consisting of the total travel time of all vehicles and excess ride-time of all users. Note that the same objectives have also been employed in the work of Parragh et al. (2009) and Molenbruch et al. (2017b) through a Pareto approach. Differently from other quality measures (e.g. total waiting time of all vehicles with passengers aboard), the consideration of excess ride-time allows to directly quantify user-specific costs. For a review on DARP problem variants and objectives, the reader is referred to Molenbruch et al. (2017a).

Approaches to solving the DARP can be categorized into two main streams, namely, approximate solution techniques and exact solution methods. Exact solution approaches for the DARP and related routing problems typically include: Branch-and-Cut algorithms (Lu and Dessouky, 2004; Cordeau, 2006; Ropke et al., 2007; Parragh, 2011; Braekers et al., 2014; Braekers and Kovacs, 2016) and Branch-and-cut-and-price algorithms (Ropke and Cordeau, 2009; Baldacci et al., 2011; Parragh and Schmid, 2013; Gschwind and Inrich, 2014). For a comprehensive review on solution methods in the DARP literature, the reader is referred to Section 4 in Molenbruch et al. (2017a). Given that the DARP is NP-hard, exact methods can only solve problems of limited size (Baugh et al., 1998; Healy and Moll, 1995; Savelsbergh, 1985). The largest problems solved for the standard DARP involved 8 vehicles and 96 customers (Ropke et al., 2007). Generalized versions of the DARP have been addressed by Braekers et al. (2014) and Parragh (2011). Braekers et al. (2014) considered heterogeneous vehicles, multiple depots, multiple user types and could solve instances of up to 8 vehicles and 80 customers. Parragh (2011) further considered a weighted-sum objective function consisting of the total routing cost and wait time for all vehicles with passengers aboard. As in this paper, the objective function included a time-dependent criterion, which in turn did not allow to reduce the problem size by avoiding timing decision variables and constraints. The problem resulted in a highly-constrained model, which could only be solved for instances of up to 4 vehicles and 40 customers.

Battery-management aspects for electric vehicles have been widely studied in several vehicle routing problems. For example, the electric and green VRP (Erdoğan and Miller-Hooks, 2012; Schneider et al., 2014; Felipe et al., 2014; Goeke and Schneider, 2015; Desaulniers et al., 2016; Pelletier et al., 2016; Keskin and Çatay, 2016; Schiffer and Walther, 2017) the hybrid electric TSP (Arslan et al., 2015; Doppstadt et al., 2016); the Mix Vehicle Routing Problem with Time Windows and recharge Stations (Baldacci et al., 2009; Hiermann et al., 2016). In Masmoudi et al. (2018), the authors propose a metaheuristic approach to solve a mixed-integer non-linear program designed for a DARP which includes electric vehicles, battery swapping stations, and the non-linear energy consumption model proposed in Genikomasakis and Mitrentsis (2017). Typical recharge policies include (1) full recharge (e.g. Schneider et al. (2014)) (2) battery swapping (e.g. Masmoudi et al. (2018)) (3) partial recharge while neglecting time windows (Felipe et al., 2014), and (4) partial recharge with no minimal battery levels imposed at the destination depots (Desaulniers et al., 2016). An assumption frequently employed in electric VRP studies is that discharge times are linearly dependent on travel times or derived from energy consumption models (Goeke and Schneider, 2015; Genikomasakis and Mitrentsis, 2017; Pelletier et al., 2018). In this study we extend the standard DARP by considering the use of electric autonomous vehicles. The extended problem is referred to as the electric Autonomous Dial-a-Ride Problem (e-ADARP). As in the work of Schneider et al. (2014) and Desaulniers et al. (2016), battery consumption is assumed to be constant and independent from the load, speed, and state-of-charge (SOC) when vehicles travel between nodes. This assumption is suitable for cases where vehicle load is negligible with respect to the curb weight of the vehicle and velocity is constant or experiences infrequent variations (Desaulniers et al., 2016; Pelletier et al., 2017). This is the case for the electric autonomous vehicles considered in this study, which are characterized by limited capacity and cruise speed. Furthermore, we assume that vehicles can visit multiple charging stations along a route, can partially recharge, and need to return with minimal battery levels at the destination depots. With respect to recharge phases, we assume the SOC linearly increases with time by means of a recharge rate. This rate can be inferred from the model presented in Pelletier et al. (2017) and applied in Pelletier et al. (2018).

While some of the features of the e-ADARP relate to the electric nature of the fleet, some are derived from considerations associated with the vehicle autonomy. In particular, autonomous vehicles can operate on a non-stop schedule and so the service is not limited by the driver's shift. Therefore, the e-ADARP does not enforce vehicle maximum route-duration constraints. This introduces savings in dead-head miles and allows for higher service levels. Additionally, providing a non-stop service eliminates the need to predefine depots from which the drivers start and end their shifts. Instead, the vehicles can exit from multiple depots and might return to a set of optional destination depots, waiting for new instructions in the next planning horizon. While multiple origin and destination depots are nowadays commonly adopted in extensions of the standard DARP (Parragh, 2011; Braekers et al., 2014), depots are normally predefined, rather than treated as a decision process. Consequently, in the e-ADARP the planning and battery-management problem is further supplemented by a vehicle-to-depot assignment problem which is not bounded by the shifts of the drivers.

To summarize, compared to classical DARP, the e-ADARP is supplemented with the following features: (1) battery-management, (2) intermediate stops for vehicle recharge, (3) vehicles may be heterogeneous in terms of capacity and initial battery inventories, (4) vehicles may be initially located at different depots, (5) vehicles may return to a set of optional depots, (5) no restrictions on maximum route-durations are applied, and (6) the total excess ride-time of users is added as a criterion in a weighted objective function. Note that, most of the mentioned features can be singularly found in the vehicle-routing literature. Nevertheless, to the best of our knowledge, their combination has not yet been explored. The combination of these features results in a new highly-constrained problem variant to be studied.

There are three primary contributions to this study. First, we introduce the e-ADARP and formulate it as a Mixed-Integer Linear Problem. Second, we devise a Branch-and-Cut algorithm and propose new problem-specific valid inequalities. Third,

we supplement benchmark instances from literature (Cordeau, 2006) with charging stations and battery specifications and provide new benchmark instances derived from real data from Uber Technologies Inc. in San Francisco. The rest of the paper is organized as follows: in Section 2 we introduce a 3-index and 2-index model for the e-ADARP; Section 3 defines several valid inequalities, including new inequalities specifically designed for the e-ADARP; a branch-and-cut framework that utilizes these valid inequalities is then introduced in Section 4; computational experiments are reported in Section 5, followed by the conclusions and future research directions in Section 6.

2. Mathematical formulations

2.1. Three-index formulation

Consider a complete directed graph $\mathbb{G} = (\mathcal{V}, \mathcal{A})$ where $\mathcal{V}$ denotes the set of vertices and $\mathcal{A}$ the set of edges. Also consider a set $\mathcal{K} = \{1, \ldots, k\}$ of electric autonomous vehicles stationed at origin depots $\{o_1, \ldots, o_k\} \in \mathcal{O}$. The vehicles are heterogeneous in terms of their capacities C^k, with total maximum vehicle capacity $C = \max_{k \in \mathcal{K}} C^k$, homogeneous in terms of their battery capacities Q, and might feature different initial battery inventories B_{o_k}. The vehicles are utilized to give service to n users, specifying their pickup locations $\mathcal{P} = \{1, \ldots, n\}$, dropoff locations $\mathcal{D} = \{n+1 \ldots, 2n\}$, and time windows $[arr_i, dep_i]$ around their desired arrival times. All user requests are known at the start of the planning period and need to be served. Furthermore, maximum user ride-times u_i are imposed to limit the time users spend on-board the vehicles. Other than the origin depots and pickup and dropoff locations, the set of vertices $\mathcal{V}$ also include charging stations $\mathcal{S}$ and optional destination depots $\mathcal{F}$. We consider that each vehicle can return to one optional destination depot in $\mathcal{F}$. Differently from the set of the origin depots $\mathcal{O}$, the cardinality of $\mathcal{F}$ might be higher than the number of vehicles and includes the nodes in $\mathcal{O}$.

Each location $i \in \mathcal{V}$ is characterized by the change in load l_i, which is positive at pickup locations, negative at dropoff locations, and is zero at all other locations. In addition, non-null service times d_i are defined at pickup and dropoff locations, which represent the time vehicles need in order to board users. The amount of energy recharged at the charging stations in $\mathcal{S}$ is proportional to the time spent at the facilities. Each charging facility $s \in \mathcal{S}$ can only be accessed by empty vehicles and is characterized by a recharge rate α_s. This rate indicates the amount of energy transferred per unit time (i.e. fast charging, slow charging). It is assumed that vehicles can partially recharge at the visited charging stations. Finally, the vehicle battery levels cannot be lower than a certain minimum SOC upon arrival at one of the optional destination depots $f \in \mathcal{F}$ by the end of the planning horizon T_p. Such battery levels are controlled by the minimum battery level ratio r.

The edges in $\mathcal{A}$ represent travel times $t_{i,j}$ between any two locations i and $j \in \mathcal{V}$. The battery consumptions $\beta_{i,j}$ can be inferred from the travel times $t_{i,j} \in \mathcal{A}$ combined with other features by means of an energy consumption model (Goeke and Schneider, 2015; Pelletier et al., 2017). We assume that the triangular inequality holds both for travel times and battery consumptions.

A binary decision variable $x^k_{i,j}$ denotes whether vehicle k sequentially visits locations i and $j \in \mathcal{V}$. T^k_i represents the time at which vehicle k begins service at location $i \in \mathcal{V}$, L^k_i represents its load after service, and B^k_i represents its battery state at the beginning of service. In addition, E^k_s denotes the recharge time of vehicle k at stations $s \in \mathcal{S}$. Finally, R_i represents the excess time of user $i \in \mathcal{P}$. The objective of the e-ADARP is to find minimum cost routes in order to serve all users while respecting time-window, capacity, and battery constraints. The cost is defined by means of a weighted objective function consisting of the total travel time of all vehicles and excess ride-time of all users. A summary of the e-ADARP problem sets, parameters, and decision variables is reported in Table 1.

Note that the parameters related to battery consumption, recharge rate, and final minimum battery level may be defined as vehicle-specific. Similarly, vehicle-specific charging stations and optional destination depots can be defined. Nevertheless, in the following models we assume that such parameters and sets are homogeneous among all vehicles. This assumption is reasonable in the employment of autonomous electric mini-buses, as nowadays such vehicles mount the same commercial batteries and do not significantly differ in terms of dimensions and weights.

A 3-index formulation for the e-ADARP, building on the DARP formulation provided in Cordeau (2006), is defined as follows:

$$(e-ADARP3) \quad \min w_1 \sum_{k \in \mathcal{K}} \sum_{i,j \in \mathcal{V}} t_{i,j} x^k_{i,j} + w_2 \sum_{i \in \mathcal{P}} R_i \tag{1}$$

subject to:

$$\sum_{j \in \mathcal{P} \cup \mathcal{S} \cup \mathcal{F}} x^k_{o^k,j} = 1 \qquad \forall k \in \mathcal{K} \tag{2}$$

$$\sum_{j \in \mathcal{F}} \sum_{i \in \mathcal{D} \cup \mathcal{S} \cup \{o^k\}} x^k_{i,j} = 1 \qquad \forall k \in \mathcal{K} \tag{3}$$

$$\sum_{k \in \mathcal{K}} \sum_{i \in \mathcal{D} \cup \mathcal{S} \cup \{o^k\}} x^k_{i,j} \leq 1 \qquad \forall j \in \mathcal{F} \cup \mathcal{S} \tag{4}$$

Table 1
Problem sets, parameters, and decision variables.

Sets	
$\mathcal{P} = \{1, \ldots, n\}$	Set of pickup locations
$\mathcal{D} = \{n+1, \ldots, 2n\}$	Set of dropoff locations
$\mathcal{N} = \mathcal{P} \cup \mathcal{D}$	Set of pickup and dropoff locations
$\mathcal{K} = \{1, \ldots, k\}$	Set of available vehicles
$\mathcal{O}$	Set of origin depots for vehicles $k \in \mathcal{K}$, the origin of vehicle k is denoted by o^k
$\mathcal{F}$	Set of all available destination depots
$\mathcal{S}$	Set of all charging stations
$\mathcal{V} = \mathcal{N} \cup \mathcal{O} \cup \mathcal{F} \cup \mathcal{S}$	Set of all possible locations
	Parameters
$t_{i,j}$	Travel time from location $i \in V$ to location $j \in \mathcal{V}$
arr_i	Earliest time at which service can begin at $i \in \mathcal{V}$
dep_i	Latest time at which service can begin at $i \in \mathcal{V}$
d_i	Service duration at location $i \in \mathcal{V}$
l_i	Change in load at location $i \in \mathcal{N}$
u_i	Maximum ride-time for customer with pickup at $i \in \mathcal{P}$
C^k	Capacity of vehicle $k \in \mathcal{K}$
Q	Effective battery capacity
B_0^k	Initial battery capacity of vehicle $k \in \mathcal{K}$
r	Final minimum battery level ratio
$\beta_{i,j}$	Battery consumption between nodes $i, j \in \mathcal{V}$
α_s	Recharge rate at charging facility $s \in \mathcal{S}$
T_p	Planning horizon
	Decision Variables
$x_{i,j}^k$	1 if vehicle k sequentially stops at location i and $j \in \mathcal{V}$, 0 otherwise.
T_i^k	Time at which vehicle k starts its service at location $i \in \mathcal{V}$
L_i^k	Load of vehicle k at location $i \in \mathcal{V}$
B_i^k	Battery load of vehicle k at location $i \in \mathcal{V}$
E_s^k	Charging time of vehicle k at charging station $s \in \mathcal{S}$
R_i	Excess ride-time of passenger $i \in \mathcal{P}$

$$\sum_{\substack{j \in \mathcal{V} \\ j \neq i}} x_{i,j}^k - \sum_{\substack{j \in \mathcal{V} \\ j \neq i}} x_{j,i}^k = 0 \qquad \forall k \in \mathcal{K}, i \in \mathcal{N} \cup \mathcal{S} \tag{5}$$

$$\sum_{k \in \mathcal{K}} \sum_{\substack{j \in \mathcal{N} \\ j \neq i}} x_{i,j}^k = 1 \qquad \forall i \in \mathcal{P} \tag{6}$$

$$\sum_{\substack{j \in \mathcal{N} \\ j \neq i}} x_{i,j}^k - \sum_{\substack{j \in \mathcal{N} \\ j \neq n+i}} x_{j,n+i}^k = 0 \qquad \forall k \in \mathcal{K}, i \in \mathcal{P} \tag{7}$$

$$T_i^k + d_i + t_{i,n+i} \leq T_{n+i}^k \qquad \forall k \in \mathcal{K}, i \in \mathcal{P} \tag{8}$$

$$arr_i \leq T_i^k \leq dep_i \qquad \forall k \in \mathcal{K}, i \in \mathcal{V} \tag{9}$$

$$T_{n+i}^k - T_i^k - d_i \leq u_i \qquad \forall k \in \mathcal{K}, i \in \mathcal{P} \tag{10}$$

$$T_i^k + t_{i,j} + d_i - M_{i,j}\left(1 - x_{i,j}^k\right) \leq T_j^k \qquad \forall k \in \mathcal{K}, i \in \mathcal{V}, j \in \mathcal{V}, i \neq j | M_{i,j} > 0 \tag{11}$$

$$R_i \geq T_{n+i}^k - T_i^k - d_i - t_{i,n+i} \qquad \forall k \in \mathcal{K}, i \in \mathcal{P} \tag{12}$$

$$L_i^k + l_j - G_{i,j}^k\left(1 - x_{i,j}^k\right) \leq L_j^k \qquad \forall k \in \mathcal{K}, i \in \mathcal{V}, j \in \mathcal{V}, i \neq j \tag{13}$$

$$L_i^k + l_j + G_{i,j}^k\left(1 - x_{i,j}^k\right) \geq L_j^k \qquad \forall k \in \mathcal{K}, i \in \mathcal{V}, j \in \mathcal{V}, i \neq j \tag{14}$$

$$L_i^k \geq \max(0, l_i) \qquad \forall k \in \mathcal{K}, \forall i \in \mathcal{N} \tag{15}$$

$$L_i^k \leq \min\left(C^k, C^k + l_i\right) \quad \forall k \in \mathcal{K}, \forall i \in \mathcal{N} \tag{16}$$

$$L_i^k = 0 \quad \forall k \in \mathcal{K}, i \in o^k \cup \mathcal{F} \cup \mathcal{S} \tag{17}$$

$$B_i^k = B_0^k \quad \forall k \in \mathcal{K}, i \in o^k \tag{18}$$

$$B_j^k \leq B_i^k - \beta_{i,j} + Q\left(1 - x_{i,j}^k\right) \quad \forall k \in \mathcal{K}, i \in \mathcal{V} \setminus \mathcal{S}, j \in \mathcal{V} \setminus \{o^k\}, i \neq j \tag{19}$$

$$B_j^k \geq B_i^k - \beta_{i,j} - Q\left(1 - x_{i,j}^k\right) \quad \forall k \in \mathcal{K}, i \in \mathcal{V} \setminus \mathcal{S}, j \in \mathcal{V} \setminus \{o^k\}, i \neq j \tag{20}$$

$$B_j^k \leq B_s^k + \alpha_s E_s^k - \beta_{s,j} + Q\left(1 - x_{s,j}^k\right) \quad \forall k \in \mathcal{K}, s \in \mathcal{S}, j \in \mathcal{P} \cup \mathcal{F} \cup \mathcal{S}, s \neq j \tag{21}$$

$$B_j^k \geq B_s^k + \alpha_s E_s^k - \beta_{s,j} - Q\left(1 - x_{s,j}^k\right) \quad \forall k \in \mathcal{K}, s \in \mathcal{S}, j \in \mathcal{P} \cup \mathcal{F} \cup \mathcal{S}, s \neq j \tag{22}$$

$$Q \geq B_s^k + \alpha_s E_s^k \quad \forall k \in \mathcal{K}, s \in \mathcal{S} \tag{23}$$

$$B_i^k \geq rQ \quad \forall k \in \mathcal{K}, i \in \mathcal{F} \tag{24}$$

$$E_s^k \leq T_s^k - t_{i,s} - T_i^k + M_{i,s}^k\left(1 - x_{i,s}^k\right) \quad \forall k \in \mathcal{K}, \forall s \in \mathcal{S}, i \in \mathcal{D} \cup \mathcal{S} \cup \{o^k\}, i \neq s \tag{25}$$

$$E_s^k \geq T_s^k - t_{i,s} - T_i^k - M_{i,s}^k\left(1 - x_{i,s}^k\right) \quad \forall k \in \mathcal{K}, \forall s \in \mathcal{S}, i \in \mathcal{D} \cup \mathcal{S} \cup \{o^k\}, i \neq s \tag{26}$$

$$x_{i,j}^k \in \{0, 1\} \quad \forall k \in \mathcal{K}, i \in \mathcal{V}, j \in \mathcal{V} \tag{27}$$

$$B_i^k \geq 0 \quad \forall k \in \mathcal{K}, i \in \mathcal{V} \tag{28}$$

$$E_s^k \geq 0 \quad \forall k \in \mathcal{K}, s \in \mathcal{S} \tag{29}$$

Constraints (2) ensure that all vehicles exit their origin depots and visit a pickup location $\mathcal{P}$, relocate to a charging station $\mathcal{S}$, or proceed to a destination depot $\mathcal{F}$. Constraints (3) guarantee that all vehicles return to a selected destination depot. Note that, since $\mathcal{F}$ also includes the origin depots $\mathcal{O}$, a non-utilized vehicle travels between its origin depots $o^k \in \mathcal{O}$ and its geographically coincident destination depot $\bar{o}^k \in \mathcal{F}$. Therefore, cases where $x_{o^k,\bar{o}^k}^k = 1$ imply that vehicle k is not being used. Constraints (4) allow each optional destination depot and charging station to be visited at most once. Such locations can be replicated in order to allow multiple visits to the nodes in $\mathcal{F}$ and $\mathcal{S}$. Flow conservation is ensured by constraints (5). Constraints (6)–(7) ensure that every pickup location is visited exactly once and that each pickup and dropoff pair is served by the same vehicle.

Timing constraints are added to define service start times and excess ride-times. Though not explicitly denoted by decision variables, waiting can occur at any location and can be retrieved through post-processing. Constraints (8) guarantee that each pickup location i is visited before its dropoff location $n+i$, by means of the direct travel time between the two locations and service time at location i. Constraints (9) set time windows around the beginning of service at each location and constraints (10) impose maximum ride-times for the users. Constraints (11) set a lower bound on the service start time at location $j \in \mathcal{V}$, which is visited right after location $i \in \mathcal{V}$, where $M_{i,j} = \max\{0, dep_i + d_i + t_{i,j} - arr_j\}$. Constraints (12) calculate the excess ride-time for user i, where the ideal travel time $t_{i,n+i} + d_i$ of user $i \in \mathcal{P}$ is subtracted from the actual travel time $T_{n+i}^k - T_i^k$.

Load conservation and capacity constraints are added to track loads and ensure capacities of all vehicles are not exceeded. We assume that charging stations can only be visited when vehicles are empty. In constraints (13) and (14), the load at location $j \in \mathcal{V}$ is computed from the load at the preceding location $i \in \mathcal{V}$ and the change in load at location j, where $G_{i,j}^k = \min\{C^k, C^k + l_i\}$. Constraints (14) are redundant with respect to the model formulation. However, they help strengthening the LP relaxations. Constraints (15) and (16) set lower and upper bounds on the occupancy of all vehicles and constraints (17) ensure that vehicles are empty at depots and charging stations. battery-management constraints are introduced to track battery levels when traveling between locations and during recharge phases. Furthermore, vehicles have initial battery levels and need to have minimum battery levels at the end of the planning horizon. Constraints (18) set initial battery levels for vehicles at origin depots o^k. Constraints (19) and (20) set the battery level state from any location $i \in V \setminus \mathcal{S}$ to any

location $j \in V \backslash o(k)$, while constraints (21) and (22) set the battery level state after a visit to a charging facility $s \in \mathcal{S}$ to any location $j \in \mathcal{P} \cup \mathcal{F} \cup \mathcal{S}$. Constraints (23) set upper bounds on the battery level states at charging stations while constraints (24) impose minimum battery levels for all vehicles returning to the depots. Constraints (25) and (26) define upper and lower bounds on the recharge time at charging station $s \in S$. Integrality and non-negativity constraints are set in (27)–(29).

2.2. Two-index formulation

In this section we present a 2-index mathematical formulation for the e-ADARP. Note that, although 2-index-based branch-and-cut algorithms typically outperform 3-indexed frameworks (Ropke et al., 2007; Parragh, 2011; Braekers et al., 2014), a 3-index formulation for the e-ADARP becomes necessary when considering vehicle-dependent battery consumptions and recharge rates.

The main limitation when transforming a 3-index formulation into a 2-index formulation is that the decision variables do not feature an index k representing the vehicles and, as a result, vehicle-specific constraints can no longer be directly modeled. Nevertheless, violations of pairing, precedence, and capacity considerations can be prevented by introducing a set of exponential constraints which are then separated during the search, as first presented by Ruland and Rodin (1997) and later applied by Ropke et al. (2007), Parragh (2011), and Braekers et al. (2014). Both multiple depots and heterogeneity in terms of capacity and initial battery inventories can be modeled by considering a singular common artificial origin and destination depot $\{0, 2n+1\}$ and by representing $\mathcal{O}$ and $\mathcal{F}$ as dummy origin and destination depots respectively (Baldacci et al., 2009; Parragh, 2011; Braekers et al., 2014)). As a result, in the 2-index formulation, the vertex set $\mathcal{V}$ consists of sets $\{0, 2n+1\}, \mathcal{P}, \mathcal{D}, \mathcal{O}, \mathcal{F}, \mathcal{S}$. As in Braekers et al. (2014) several arcs (i, j) are eliminated from the arc set $\mathcal{V}$ to ensure that each route starts with a dummy origin depot and ends at a dummy destination depot. Therefore, the following arcs (i, j) are eliminated from the complete graph $\mathbb{G}$:

$$(i, 0), (2n+1, i) \quad \forall i \in \mathcal{V}$$

$$(0, j) \quad \forall j \in \mathcal{V} \setminus \mathcal{O}$$

$$(i, 2n+1) \quad \forall i \in \mathcal{V} \setminus \mathcal{F}$$

To impose precedence and pairing constraints, $\mathbb{I}$ denotes the set of all vertex subsets $\mathcal{I} \subseteq \mathcal{V} \setminus \mathcal{S}$ such that $0 \in \mathcal{I}, 2n+1 \notin \mathcal{I}$ and there is at least one vertex i for which $i \notin \mathcal{I}$ and $n+i \in \mathcal{I}$. $\bar{\mathbb{I}}$ denotes the complementary set of $\mathbb{I}$ with $\mathcal{S} \not\subset \bar{\mathcal{I}}, \ \forall \bar{\mathcal{I}} \in \mathbb{I}$. Then, given precedence and paring considerations between i and $n+i$, sets $\mathcal{I} \in \mathbb{I}$ need to be exited at least once. Given that charging stations are not included in $\mathbb{I}$ or $\bar{\mathbb{I}}$, and that at least one arc needs to directly exit $\mathcal{I} \in \mathbb{I}$ towards $\bar{\mathcal{I}} \in \bar{\mathbb{I}}$, precedence and pairing constraints also prevent non-empty vehicles from entering charging stations $\mathcal{S}$. Capacity constraints can be enforced by setting a lower bound on the number of times vehicles must enter and exit $\mathcal{I}$ by computing $\max\{1, \lceil \frac{|\sum_{i \in \mathcal{I}} l_i|}{C} \rceil\}$ (Ropke et al., 2007).

After visiting a dummy depot, capacities are set such that they correspond to their actual levels, as presented in Braekers et al. (2014). Therefore $l_i = C - C^k \ \ \forall i \in \mathcal{O}$ and $l_i = C^k - C \ \ \forall i \in \mathcal{F}$. The vehicle battery levels are instead set to the initial battery inventories B_{o_k} at every origin depot $o_k \in \mathcal{O}$. Note that $t_{0,j} = 0 \ \ \forall j \in \mathcal{O}$.

The e-ADARP can be formulated as the following MILP:

$$(e-ADARP2) \quad \min w_1 \sum_{i,j \in \mathcal{V}} t_{i,j} x_{i,j} + w_2 \sum_{i \in \mathcal{P}} R_i \tag{30}$$

subject to:

$$\sum_{j \in \mathcal{O}} x_{0,j} = |\mathcal{K}| \tag{31}$$

$$\sum_{i \in \mathcal{F}} x_{i,2n+1} = |\mathcal{K}| \tag{32}$$

$$\sum_{i \in \mathcal{D} \cup \mathcal{S} \cup \mathcal{O}} x_{i,j} \leq 1 \quad \forall j \in \mathcal{F} \cup \mathcal{S} \tag{33}$$

$$\sum_{j \in \mathcal{N}} x_{i,j} = 1 \quad \forall i \in \mathcal{P} \tag{34}$$

$$\sum_{j \in \mathcal{V}} x_{i,j} - \sum_{j \in \mathcal{V}} x_{j,i} = 0 \quad \forall i \in \mathcal{N} \cup \mathcal{S} \cup \mathcal{O} \tag{35}$$

$$\sum_{i,j \in \mathcal{I}} x_{i,j} \leq |\mathcal{I}| - 2 \quad \forall \mathcal{I} \in \mathbb{I} \tag{36}$$

$$\sum_{i,j\in\mathcal{I}} x_{i,j} \leq |\mathcal{I}| - \max\left\{1, \left\lceil \frac{|\sum_{i\in\mathcal{I}} l_i|}{C} \right\rceil \right\} \quad \forall \mathcal{I} \in \mathbb{I} \tag{37}$$

$$T_i + d_i + t_{i,n+i} \leq T_{n+i} \quad \forall i \in \mathcal{P} \tag{38}$$

$$arr_i \leq T_i \leq dep_i \quad \forall i \in \mathcal{V} \tag{39}$$

$$T_{n+i} - T_i - d_i \leq u_i \quad \forall i \in \mathcal{P} \tag{40}$$

$$T_i + t_{i,j} + d_i - M_{i,j}(1 - x_{i,j}) \leq T_j \quad \forall i \in \mathcal{V}, j \in \mathcal{V}, i \neq j | M_{i,j} > 0 \tag{41}$$

$$R_i \geq T_{n+i} - T_i - d_i - t_{i,n+i} \quad \forall i \in \mathcal{P} \tag{42}$$

$$B_j \leq B_i - \beta_{i,j} + Q\left(1 - x_{i,j}\right) \quad \forall i \in \mathcal{V} \setminus \mathcal{S} \cup \{0\}, j \in \mathcal{V} \setminus \mathcal{O} \cup \{0\}, i \neq j \tag{43}$$

$$B_j \geq B_i - \beta_{i,j} - Q\left(1 - x_{i,j}\right) \quad \forall i \in \mathcal{V} \setminus \mathcal{S} \cup \{0\}, j \in \mathcal{V} \setminus \mathcal{O} \cup \{0\}, i \neq j \tag{44}$$

$$B_j \leq B_s + \alpha_s E_s - \beta_{s,j} + Q\left(1 - x_{s,j}\right) \quad \forall s \in \mathcal{S}, j \in \mathcal{P} \cup \mathcal{F} \cup \mathcal{S}, s \neq j \tag{45}$$

$$B_j \geq B_s + \alpha_s E_s - \beta_{s,j} - Q\left(1 - x_{s,j}\right) \quad \forall s \in \mathcal{S}, j \in \mathcal{P} \cup \mathcal{F} \cup \mathcal{S}, s \neq j \tag{46}$$

$$E_s \leq T_s - t_{i,s} - T_i + M_{i,s}(1 - x_{i,s}) \quad \forall s \in \mathcal{S}, i \in \mathcal{D} \cup \mathcal{S} \cup \mathcal{O}, i \neq s \tag{47}$$

$$E_s \geq T_s - t_{i,s} - T_i - M_{i,s}(1 - x_{i,s}) \quad \forall s \in \mathcal{S}, i \in \mathcal{D} \cup \mathcal{S} \cup \mathcal{O}, i \neq s \tag{48}$$

$$Q \geq B_s + \alpha_s E_s \quad \forall s \in \mathcal{S} \tag{49}$$

$$B_i \geq rQ \quad \forall i \in \mathcal{F} \tag{50}$$

$$x_{i,j} \in \{0, 1\} \quad \forall i \in \mathcal{V}, j \in \mathcal{V} \tag{51}$$

$$B_i \geq 0 \quad \forall i \in \mathcal{V} \tag{52}$$

$$E_s \geq 0 \quad \forall s \in \mathcal{S} \tag{53}$$

Note that the second criterion in the objective function (30) depends on scheduling decisions. Therefore, timing decision variables and constraints cannot be omitted from the 2-index model for the e-ADARP. Differently from the 3-index model presented in the previous section, the artificial origin and destination depots $\{0, 2n+1\}$ are exited/entered $|\mathcal{K}|$ times. As with the charging stations $\mathcal{S}$, each node in $\mathcal{F}$ may be visited at most once, as shown in constraints (33). Nevertheless, the interaction with constraints (32) and constraints (35) impose that at least $|\mathcal{K}|$ arcs enter and exit $\mathcal{F}$. Precedence and pairing constraints are imposed by inequalities (36), whereas rounded capacity constraints are given in (37). As noted in Ropke et al. (2007), since $\sum_{i,j\in\mathcal{I}} x_{i,j} = |\mathcal{I}| - 1 - \sum_{i\in\mathcal{I}}\sum_{i\in\bar{\mathcal{I}}} x_{i,j}$, precedence constraints (36) can be equivalently written as $\sum_{i\in\mathcal{I}}\sum_{i\in\bar{\mathcal{I}}} x_{i,j} \geq 1 \quad \forall \mathcal{I} \in \mathbb{I}$. Finally, given that each node can be visited by one vehicle only, the remaining constraints (38)–(53) are equivalent to constraints (8)–(29).

3. Valid inequalities

In this section, we introduce several families of valid inequalities used in order to strengthen the e-ADARP formulations. In Section 3.1, we present sets of valid inequalities that are adopted from the vehicle routing literature. Then, in Section 3.2, we discuss several sets of valid inequalities that are specifically designed by taking into account properties of the e-ADARP.

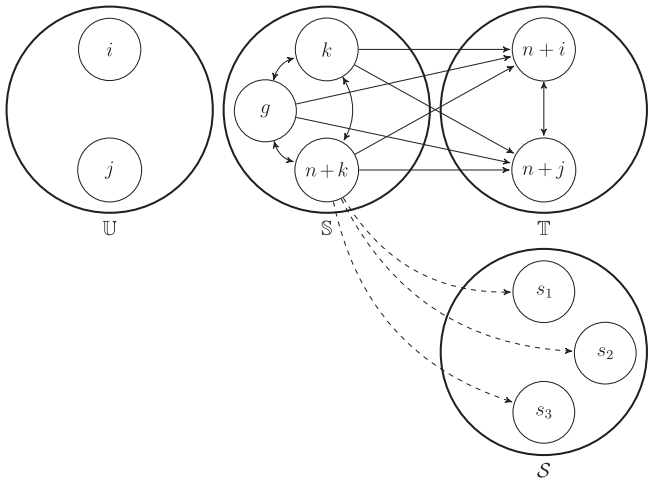

Fig. 1. Inequalities (55) for the case in which $\mathbb{U} = \{i, j\}$, $\mathbb{S} = \{k, g, n+k\}$, $\mathbb{T} = \{n+i, n+j\}$, and $\mathcal{S} = \{s_1, s_2, s_3\}$.

3.1. Valid inequalities from the vehicle routing literature

Several families of valid inequalities from the vehicle routing literature are also valid for the e-ADARP and can be lifted to account for the charging stations. In particular, the following inequalities can be directly applied to the e-ADARP: (1) time-window strengthening (Cordeau (2006)), (2) incompatible users constraints (Cordeau (2006)), (3) generalized order constraints (Ruland and Rodin (1997);Cordeau (2006)), (4) subtour elimination constraints (Cordeau (2006)) (Note that subtours can also include the charging stations), (5) strengthened capacity constraints (Ropke et al. (2007)), (6) infeasible path constraints based on maximum ride-time considerations (Cordeau (2006)), (7) tournament constraints (Ascheuer et al., 2000; Ropke et al., 2007), (8) fork constraints (Ropke et al., 2007), and (9) reachability constraints (Lysgaard, 2006; Ropke et al., 2007).

In the case of the e-ADARP, capacity constraints can be lifted considering the recharge stations. This set of constraints is added to prevent situations in which the number of vehicles visiting set $\mathbb{S} \subseteq \mathcal{N}$ is not sufficient to accommodate its demand. Considering $C = \max_{k \in \mathcal{K}} C$, and letting $\mathbb{S}, \mathbb{T} \subseteq \mathcal{N}$ be two disjoint sets such that $\sum_{i \in \mathbb{S}} l_i > 0$, and $\mathbb{U} = \pi(\mathbb{T}) \setminus (\mathbb{S} \cup \mathbb{T})$, where $\pi(\mathbb{T}) = \{i \in \mathcal{P} | n+i \in \mathbb{T}\}$, capacity constraints can be written as follows (Ropke et al., 2007):

$$x(\mathbb{S}) + x(\mathbb{T}) + x(\mathbb{S} : \mathbb{T}) \leq |\mathbb{S}| + |\mathbb{T}| - \left\lceil \frac{l(\mathbb{S}) + l(\mathbb{U})}{C} \right\rceil \tag{54}$$

In the case of the e-ADARP, charging stations can only be accessed when vehicles are unloaded (17) and each node can be exited at most once. Therefore, capacity constraints can be lifted considering arcs from dropoff locations in $\mathbb{S}$ to the set of stations $\mathcal{S}$, as follows:

$$x(\mathbb{S}) + x(\mathbb{T}) + x(\mathbb{S} : \mathbb{T}) + x((\mathbb{S} \cap \mathcal{D}) : \mathcal{S}) \leq |\mathbb{S}| + |\mathbb{T}| - \left\lceil \frac{l(\mathbb{S}) + l(\mathbb{U})}{C} \right\rceil \tag{55}$$

Fig. 1 shows an illustrative example of inequalities (55) for the case in which $\mathbb{U} = \{i, j\}$, $\mathbb{S} = \{k, g, n+k\}$, $\mathbb{T} = \{n+i, n+j\}$, and $\mathcal{S} = \{s_1, s_2, s_3\}$.

3.2. Valid inequalities for the e-ADARP

The following valid inequalities are based on battery-management aspects introduced in the e-ADARP. In Sections 3.2.1 and 3.2.2 we present infeasible path constraints that consider battery capacity and load restrictions at charging stations respectively. We note that in both cases, the resulting constraints can be presented in the structure of tournament constraints and used in the generation of fork constraints (Ropke et al., 2007).

3.2.1. Infeasible path inequalities – Battery capacity

Similar to the maximum ride-time constraints introduced in Cordeau (2006), it is possible to introduce a set of infeasible path inequalities related to battery-management. The vehicles considered in this study are electric. As such, they need to have enough battery to perform partial paths without recharge. Consider a path $\mathbb{P} = \{s', i, m_1, m_2, \ldots, m_q, n+i, s''\}$, such that $\mathcal{H} = \{m_1, m_2, \ldots, m_q\} \subseteq \mathcal{N}$, $i \in \mathcal{P}$, and $\{s', s''\} \in \mathcal{S}$. In terms of battery consumption, s' is the closest charging station to location i and s'' is the closest station to $n+i$, i.e. $s' = \arg\min_{s \in \mathcal{S}} \beta_{s,i}$ and $s'' = \arg\min_{s \in \mathcal{S}} \beta_{n+i,s}$. Assuming that the triangular inequality for battery consumption holds, and considering the effective battery capacity Q, we deem path $\mathbb{P}$ to be infeasible if

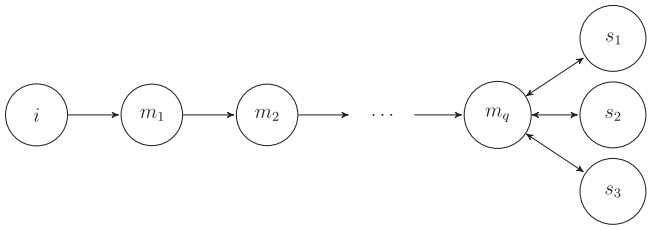

Fig. 2. Inequalities (57) for the case in which $\mathbb{P} = \{i, m_1, m_2, \ldots, m_q, s_2\}$ and $|\mathcal{S}| = 3$.

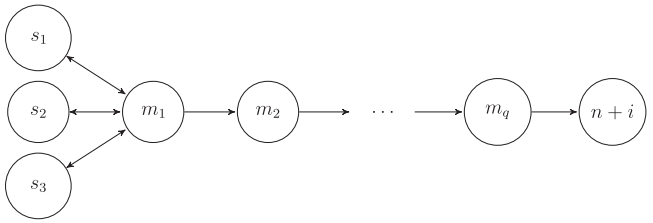

Fig. 3. Inequalities (58) for the case in which $\mathbb{P}'' = \{s_2, m_1, m_2, \ldots, m_1, n+i\}$ and $|\mathcal{S}| = 3$.

the battery consumption required to traverse it is greater than Q. That is, if $\beta_{s',i} + \beta_{i,m_1} + \sum_{h=1}^{q-1} \beta_{m_h,m_{h+1}} + \beta_{m_p,n+i} + \beta_{n+i,s''} > Q$.

Next, vehicles need to return to destination depots having some minimum battery levels, which depend on the minimal battery level ratio r. Then, assuming that the destination depot $f \in \mathcal{F}$ is chosen such that the battery consumption from $n+i$, i.e. $f = \arg\min_{f\in\mathcal{F}} \beta_{n+i,f}$, is minimized if $\beta_{s',i} + \beta_{i,m_1} + \sum_{h=1}^{q-1} \beta_{m_h,m_{h+1}} + \beta_{m_p,n+i} + \beta_{n+i,f} > (1-r)Q$, path $\mathbb{P}' = \{s', i, m_1, m_2, \ldots, m_q, n+i, f\}$ is infeasible.

Furthermore, vehicles start their service with some initial battery level B_{o_k}. Assuming the maximum initial SOC is set to $B_{o_{\max}} = \max\ nolimits_{k\in\mathcal{K}} B_{o_k}$, and the origin depot $o_k \in \mathcal{O}$ is chosen such that it minimizes battery consumption to i, i.e. $o = \arg\min_{o_k\in\mathcal{O}} \beta_{o_k,i}$. Then, if $\beta_{o,i} + \beta_{i,m_1} + \sum_{h=1}^{q-1} \beta_{m_h,m_{h+1}} + \beta_{m_q,n+i} + \beta_{n+i,s''} > B_{o_{\max}}$, path $\mathbb{P}'' = \{o, i, m_1, m_2, \ldots, m_q, n+i, s''\}$ is infeasible.

Finally, let $\mathcal{A}(\mathcal{H})$ be the edges of $\mathcal{H}$. Then, if all paths $\mathbb{P}$, $\mathbb{P}'$, and $\mathbb{P}''$ are infeasible, path $(i, \mathcal{H}, n+i)$ can be eliminated by the following inequalities (Cordeau, 2006):

$$x_{i,m_1} + \sum_{h=1}^{q-1} x_{m_h,m_{h+1}} + x_{m_q,n+i} \leq q - 1 \tag{56}$$

3.2.2. Infeasible path inequalities – Charging stations "Walls"

Recall that, in the e-ADARP, vehicles are not allowed to visit charging stations with passengers on board (17). Therefore, any visit to a charging station between the pickup of a customer and its dropoff is infeasible. Consider a path $\mathbb{P}'$ connecting the pickup location of user i and a charging station s by a sequence of q intermediate locations $\{m_1, m_2, \ldots, m_q\}$ with $m_{1,\ldots,q} \in \mathcal{P} \cup \mathcal{D} \setminus \{n+i\}$. Note that visits to charging stations are only possible when vehicles are empty, in a feasible integer solution, at most q arcs can be selected from path $\mathbb{P}'$. These inequalities can be further lifted by including arcs connecting the charging stations $s \in \mathcal{S}$ to the last intermediate location m_q, and from m_q to s, as follows:

$$x_{i,m_1} + \sum_{h=1}^{q-1} x_{m_h,m_{h+1}} + \sum_{s\in\mathcal{S}} \left(x_{m_q,s} + x_{s,m_q}\right) \leq q \tag{57}$$

An illustrative example for inequalities (57) for the case in which $\mathbb{P} = \{i, m_1, m_2, \ldots, m_q, s_2\}$ and $|\mathcal{S}| = 3$ is given in Fig. 2.

Similarly, infeasible path inequalities (58) are derived by considering a path $\mathbb{P}''$ connecting a charging station s to a dropoff location $n+i$ by a sequence of q intermediate locations $\{m_1, m_2, \ldots, m_q\}$ with $m_{1,\ldots,q} \in \mathcal{D} \cup \mathcal{P} \setminus \{i\}$.

$$\sum_{s\in\mathcal{S}} (x_{s,m_1} + x_{m_1,s}) + \sum_{h=1}^{q-1} x_{m_h,m_{h+1}} + \sum_{s\in\mathcal{S}} x_{m_q,n+i} \leq q \tag{58}$$

An illustrative example for inequalities (58) for the case in which $\mathbb{P}'' = \{s_2, m_1, m_2, \ldots, m_q, n+i\}$ and $|\mathcal{S}| = 3$ is given in Fig. 3.

3.2.3. Charging stations and time windows constraints

We derive a set of constraints that reflect the interaction between charging stations and time windows. Suppose a vehicle leaves by the earliest time from $n+i \in \mathcal{D}$, recharges at $s \in \mathcal{S}$, and travels to $j \in \mathcal{P}$. Then, in order to justify the deviation from

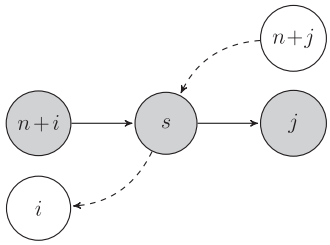

Fig. 4. Inequalities (59): Charging stations and time windows constraints.

$n+i$ to s before reaching j, the vehicle needs to recharge for a minimum time. This time can be inferred from the battery consumptions between $n+i$, s, j and the recharge rate α_s, as $\frac{\beta_{n+i,s}+\beta_{s,j}-\beta_{n+i,j}}{\alpha_s}$. Then, if path $\{n+i,s,j\}$ is infeasible with respect to its start and end time windows, i.e. $t_{n+i,s}+d_{n+i}+t_{s,j}+\frac{\beta_{n+i,s}+\beta_{s,j}-\beta_{n+i,j}}{\alpha_s} > dep_j - arr_{n+i}$, the following infeasible path inequalities are identified:

$$x_{n+i,s}+x_{s,j}+x_{n+j,s} \leq 1 \qquad \forall i \in \mathcal{P}, j \in \mathcal{N}$$

Next, suppose the same vehicle travels from $n+j$ to station s and then reaches i. In this case, compute a minimum recharge time $\frac{\beta_{n+j,s}+\beta_{s,i}-\beta_{n+j,i}}{\alpha_s}$ at station s. Then, if both paths $\{n+i,s,j\}$ and $\{n+j,s,i\}$ are violated, i.e. $t_{n+i,s}+d_{n+i}+t_{s,j}+\frac{\beta_{n+i,s}+\beta_{s,j}-\beta_{n+i,j}}{\alpha_s} > dep_j - arr_{n+i}$ and $t_{n+j,s}+d_{n+j}+t_{s,i}+\frac{\beta_{n+j,s}+\beta_{s,i}-\beta_{n+j,i}}{\alpha_s} > dep_i - arr_{n+j}$, stronger inequalities can be added as follows:

$$x_{n+i,s}+x_{s,j}+x_{n+j,s}+x_{s,i} \leq 1 \qquad \forall i \in \mathcal{P}, j \in \mathcal{N} \tag{59}$$

An illustrative example for inequalities (59) is given in Fig. 4.

3.2.4. Charging visits constraint

In the e-ADARP, one can set a lower bound on the minimal number of visits to charging stations by considering the total amount of battery consumed by all vehicles during service. On the left hand-side of inequality (60), the number of times the vehicles fully discharge with respect to the effective battery capacity Q is computed. Note each vehicle starts and ends service with positive battery levels. For this reason, the total maximal initial SOC $B_{o_{\max}}$ for all utilized vehicles (i.e. all vehicles k with $x_{o^k,\bar{o}^k}=0$) is deducted from the left-hand side, while the total final SOC for all utilized vehicles is added back to the left-hand-side of inequality (60). On the right-hand side of inequalities (60), the sum represents the minimum number of times all vehicles exit charging stations, i.e. the minimum number of visits to charging stations.

$$\sum_{i,j\in\mathcal{V},i\neq j}\frac{\beta_{i,j}x_{i,j}}{Q}-\left(|\mathcal{K}|-\sum_{i\in\mathcal{O}}\sum_{j\in\bigcup_{k\in\mathcal{K}}\{\bar{o}^k\}}x_{i,j}\right)\left(\frac{B_{o_{max}}}{Q}-r\right)\leq\sum_{s\in\mathcal{S}}\sum_{i\in\mathcal{P}\cup\mathcal{S},i\neq s}x_{s,i} \tag{60}$$

Note that inequality (60) is inspired by a similar concept in the context of the locomotive refuelling problem (Raviv and Kaspi (2012)). The constraint is also similar to the rounded capacity constraints introduced in Cordeau (2006) where, in place of passenger capacity and loads, total battery consumption and visits to stations are considered. Finally, note that for the 3-index model, inequality (60) can be vehicle-specific.

4. Branch-and-Cut algorithm

The following sections present the branch-and-cut framework developed for the e-ADARP. In Section 4.1, we discuss the steps taken at the initialization of the algorithm. These include pre-processing procedures and the enumeration of several sets of inequalities. In Section 4.2, we describe the separation heuristics designed to identify violated valid inequalities as well as capacity, precedence, and paring constraints (36) and (37).

4.1. Initialization

In order to reduce the size of the problem and strengthen the LP relaxation, several steps are taken before solving the root node. These steps include time-window tightening, arc elimination, variable fixing, symmetry breaking, and the enumeration of several sets of valid inequalities. Most of these steps are based on considerations arising from standard DARP properties. For the sake of brevity, we omit the description of these initialization steps and refer the reader to Sections 5.1 and 5.2 in Cordeau (2006). Note that precedence, paring, and capacity constraints (36) and (37) may be also included at the root node by means of the separation heuristics described in Section 4.2. In the following paragraphs, we focus our discussion on considerations related to charging stations.

By definition, vehicles are required to enter charging stations with no users on board. Consequently, a visit to a charging station cannot be preceded by a pickup node and cannot be followed by a dropoff node. Specifically, arcs (i, s) with $i \in \mathcal{P}$ and $s \in \mathcal{S}$ and arcs (s, j) with $j \in \mathcal{D}$ are eliminated, as follows:

$$(i, j) \qquad \forall i \in \mathcal{O} \cup \mathcal{S}, j \in \mathcal{D}$$

$$(i, j) \qquad \forall i \in \mathcal{P}, j \in \mathcal{F} \cup \mathcal{S}$$

Next, charging stations may be visited at any time. That is, the time windows imposed at charging stations include the entire planning horizon. Some minor tightening of these time windows may be achieved by taking into account traveling times from the origin and to the destination depots. Namely, the earliest time to start service at charging station s can be set to $arr_s = \min_{o_k \in \mathcal{O}}(arr_{o_k} + t_{o_k,s})$, and similarly, the latest time to start service at charging station s can be set to $\max_{f \in \mathcal{F}}(T_p - t_{s,f})$. Finally, symmetry breaking constraints can be introduced when stations are replicated to allow for more than a single charging visit. In particular, a visit is allowed only if all preceding visits have been made. Namely, denoting by $\bar{\mathcal{S}}$ the original set of stations nodes and by m the number of station visit replications, the following symmetry breaking constraints are introduced:

$$\sum_{i \in \mathcal{O} \cup \mathcal{S} \cup \mathcal{D}} x_{i,s+j|\bar{\mathcal{S}}|} \geq \sum_{i \in \mathcal{O} \cup \mathcal{S} \cup \mathcal{D}} x_{i,s+(j+1)|\bar{\mathcal{S}}|} \qquad \forall s \in \bar{\mathcal{S}}, j = \{0, \ldots, (m-1)\} \tag{61}$$

Next, we describe some of the valid inequalities proposed in Section 3 for the e-ADARP, which are enumerated during the pre-processing step. The infeasible path constraints presented in Section 3.2.3 are of polynomial size and are fully enumerated at the root node. The charging visits constraint presented in Section 3.2.4 is also inserted at the root node. In addition, we introduce special cases of (57) and (58). Specifically, we enumerate the following sets, considering paths $\{i, j, s\}$, where $i \in \mathcal{P},\ j \in \mathcal{D} \setminus \{n+i\},\ s \in \mathcal{S}$:

$$x_{i,j} + \sum_{s=\mathcal{S}} x_{j,s} \leq 1 \qquad \forall i \in \mathcal{P}, j \in \mathcal{D}, j \neq n+i$$

And, considering paths $\{s, j, n+i\}$, where $i \in \mathcal{P},\ j \in \mathcal{P} \setminus \{i\},\ s \in \mathcal{S}$:

$$\sum_{s \in \mathcal{S}} x_{s,j} + x_{j,n+i} \leq 1 \qquad \forall i \in \mathcal{P}, j \in \mathcal{P}, j \neq i$$

Finally, for every user $i \in \mathcal{P}$ and charging station $s \in \mathcal{S}$, we generate infeasible path constraints, as follows:

$$x_{n+i,s} + x_{s,i} \leq 1 \qquad \forall i \in \mathcal{P}, s \in \mathcal{S}$$

4.2. Separation heuristics

In this section we present the separation heuristics used in the branch-and-cut algorithm. Precedence and pairing constraints (36) are separated using similar separation heuristics as those presented in Parragh (2011), where the Ford-Fulkerson algorithm is implemented to solve the max-flow problems. Rounded capacity constraints (37) are detected through an enumerative procedure: From every origin depot in $\mathcal{O}$ we extend paths along the arcs with the maximum flow $x_{i,j}$ until capacity is violated or one destination depot has been reached.

To search for violations of generalized order constraints and strengthened capacity constraints (54)–(55), we adopt the separation heuristics described in Section 4 in Ropke et al. (2007). Reachability constraints are also separated as per Ropke et al. (2007). Note that, in the e-ADARP sets A_i^+ and A_i^- also need to include arcs to/from charging stations. Moreover, since nodes $s \in \mathcal{S}$ can only be accessed by empty vehicles, sets A_i^+ and A_i^- do not contain arcs from pickups to charging stations or from stations to dropoff locations.

Subtour elimination constraints, tournament constraints with respect to time windows, maximum ride-time, and battery-management constraints are separated by the use of a greedy construction heuristic. For each pickup node $i \in \mathcal{P}$, we initialize a path with node i and iteratively append nodes to the path, such that the value of the added arc is maximized. This iterative procedure is terminated when one of the following conditions are met: (1) the next node to be appended is a destination depot $f \in \mathcal{F}$, (2) The next node to be appended already exists in the path, or (3) The path length exceeds a pre-defined value. If the construction of a path is terminated due to a repetition of a node, a subtour may have been identified. As such, in this instance, we check for violations of the subtour elimination constraints introduced in Cordeau (2006). During the construction of the path, we check both whether time-window constraints are violated for the last node appended to the path and whether the value of the relaxed solution violates tournament constraints (Ropke et al., 2007). If a tournament constraint is not identified (i.e. the backbone path is feasible), we search for violations of fork constraints using the search heuristics presented in Ropke et al. (2007). Infeasible path inequalities with respect to maximum ride-time and battery-management constraints are examined only when the constructed path includes the dropoff node $n+i$ of seed node i and does not include any charging station. For such paths, if the travel time exceeds the maximum ride-time of user i, or the three battery consumption conditions presented in Section 3.2.1 are met, we check for violations of inequalities (56).

Infeasible paths due to load considerations at the charging stations (57) and (58) are identified by using a heuristic which iteratively considers a node $s \in \mathcal{S}$ and constructs paths forwards or backwards by appending the node with maximal

flow. Specifically, in order to identify inequalities (57) we construct paths from node s forwards, whereas for inequalities (58) we construct paths to node s backwards. To search for violations of inequalities (57) we then check whether each path originating from s contains the dropoff of a user $n+j$ but not its pickup j. Similarly, to search for violations of inequalities (58) we check whether each path terminating at s contains the pickup of a user j but not its dropoff $n+j$. The search is interrupted when one of the following conditions is met: (1) a violation of inequalities (57) and (58) is identified; or (2) the forward or backward path reaches a charging facility, a dummy origin, or destination depot without violating inequalities (57) and (58).

5. Computational experiments

In this section, we present numerical experiments designed to examine the performance of the proposed e-ADARP formulations and branch-and-cut algorithm. All programs are implemented in Julia 0.7.0 using the JuMP modeling language (Dunning et al., 2017) and the MILP solver Gurobi 7.0.1 on a 3.60 GHz Intel(R) Core(TM) with 16 Gb of RAM.

5.1. Test instances

Two sets of instances are tested in the experiment: (1) Instances obtained by supplementing DARP benchmark instances from Cordeau (2006) with e-ADARP-related parameters, and (2) Instances based on ride-sharing data from Uber Technologies Inc. in 2011.

The instances proposed by Cordeau (2006) for the standard DARP are supplemented with charging stations, battery capacities, initial SOC requirements, final SOC requirements, recharge rates, and discharge rates. A single origin and destination depot is used for all vehicles, as in the original instances. That is, vehicles are limited to a specific destination depot and cannot choose from a set of potential destination depots. The capacity of all vehicles is set to three passengers and the maximum ride-time of all users is set to 30 minutes. recharge and discharge rates are given by the autonomous-electric shuttles manufacturer Navya and are set to represent a battery autonomy of 5 hours from a nominal capacity of 16.5 kWh. Namely, the recharge and discharge rates are both set to 0.055 kWh per minute (see https://www.hevs.ch/media/document/1/fiche-technique-navettes-autonomes.pdf). For the purpose of this experiment, all vehicles are assumed to start with full battery capacity and that the amount of battery discharged on each route segment is proportional to the route's travel time. The effective battery capacity and initial battery charge are both set to 14.85 kWh. That is, vehicles are required to keep 10% of their nominal capacity at all times. Note that, with respect to the average travel time exhibited in these instances, each vehicle can visit at most approximately 20 nodes with a full effective battery capacity.

In the proposed analysis, the following convention is used for the instance names: <a/u> <number of vehicles> – <number of customers>, where "a" and "u" are used for the instances adapted from Cordeau (2006) and from Uber respectively. The characteristics of the first instances are summarized in Table 2(a). The first column presents the instance name, followed by three columns presenting the time horizon T_p, number of customers n, and the number of vehicles $|\mathcal{K}|$. The last four columns present the number of constraints and variables (before pre-processing) in the resulting 3-index (e-ADARP3) and 2-index (e-ADARP2) MILP formulations. All of the presented instances are also replicated for three final minimum battery level ratios r. In particular, we analyze the case in which all vehicles need to return to one of the optional destination depots with at least 10%, 40% and 70% battery ratio levels (i.e. r=0.1, r=0.4, r=0.7).

The second set of instances is produced by extrapolating origin/destination locations and times from ride-sharing GPS logs in the city of San Francisco (CA, USA). The dataset, shared by Uber Technologies Inc. in 2011, contains a total of 1.2 million GPS logs, registered every 4 seconds from active Uber cars during one week. The dataset is processed prior to the analysis, removing invalid records, and extracting the pickup and dropoff locations for the remaining trips. The processed dataset contains about 25,000 Uber trips made during a one-week period. The daily number of trip requests varies from 2000 to 6000. The raw dataset is obtained from the GitHub repository at https://github.com/dima42/uber-gps-analysis/tree/master/gpsdata. This study focuses on the ride-sharing requests that have been served in the Downtown/Civic Center districts. Neighborhood information is obtained through the San Francisco Enterprise GIS Program (SFGIS) on the SF OpenData website. The requests from the weekend are aggregated into one single day, by neglecting the day of the request. Instances of different size are then generated by randomly selecting users at a maximum rate of one request every 3 minutes.

The San Francisco transportation network is extracted from OpenStreetMap (OSM). Information on electric vehicle charging station locations is obtained through the Alternative Fueling Station Locator from the Alternative Fuels Data Center (AFDC) of the U.S. Department of Energy. Dijkstra's shortest path algorithm is used to compute travel times between the pickup/dropoff locations, charging stations, and origin/destination depots. The travel times are estimated without considering traffic congestion, instead assuming that vehicles travel at a constant speed of 35 km/h. In the envisioned application AVs can provide non-stop ride-sharing services. As such, origin and destination depots are assumed to coincide with the set of potential charging stations. The depots also serve as temporary parking locations to provide ride-sharing services in a sequential time-horizon framework. In these instances, each vehicle may visit a maximum of five charging stations (randomly selected from the AFDC) and consequently may choose between 5 potential destination depots. Figs. 5 and 6 show the pickup and dropoff locations, as well as their time windows, after tightening, for instances a4–16 and u4–16 respectively (i.e. 4 vehicles, 16 customers). Note that the instance shown in Fig. 6 is substantially different from the one shown in Fig. 5. In particular, all instances adapted from Cordeau (2006) and from Uber, differ as follows: (1) The pickup and dropoffs

Table 2
Benchmark Instances: (a) Instances adapted from Cordeau (2006); (b) Instances from Uber ride-shares in San Francisco, CA (USA).

				e-ADARP3		e-ADARP2	
Name	T_p [min]	n	$\|\mathcal{K}\|$	# Cons	# Vars	# Cons	# Vars
a2-16	480	16	2	19,746	2990	9904	1786
a2-20	600	20	2	29,486	4354	14,550	2526
a2-24	720	24	2	41,015	5974	20,047	3394
a3-18	360	18	3	34,447	5451	12,891	2329
a3-24	480	24	3	57,174	8949	21,081	3631
a3-30	600	30	3	87,923	13,311	31,571	5221
a3-36	720	36	3	124,084	18,537	44,087	7099
a4-16	240	16	4	35,866	5964	11,245	2140
a4-24	360	24	4	74,887	11,924	22,172	3876
a4-32	480	32	4	127,995	19,932	36,829	6124
a4-40	600	40	4	194,035	29,988	54,874	8884
a4-48	720	48	4	271,841	42,092	76,050	12156
a5-40	480	40	5	235,439	37,475	56,028	9265
a5-50	600	50	5	359,418	56,785	84,664	13515

(a)

				e-ADARP3		e-ADARP2	
Name	T_p [min]	n	$\|\mathcal{K}\|$	# Cons	# Vars	# Cons	# Vars
u2-16	127	16	2	63,296	3990	11,348	2233
u2-20	166	20	2	36,513	5546	16,216	3053
u2-24	199	24	2	50,094	7358	22,324	4001
u3-18	161	18	3	43,668	7095	13,924	2731
u3-24	188	24	3	69,947	11,025	22,291	4129
u3-30	237	30	3	104,008	15,819	33,235	5815
u3-36	280	36	3	142,511	21,477	45,619	7789
u4-16	93	16	4	47,788	7964	12,013	2427
u4-24	439	24	4	92,195	14,692	23,132	4259
u4-32	183	32	4	150,075	23,468	37,699	6603
u4-40	471	40	4	222,327	34,292	55,945	9459
u4-48	272	48	4	310,059	47,164	78,097	12827
u5-40	211	40	5	275,315	42,855	57,151	9655
u5-50	284	50	5	409,514	63,365	84,991	13985

(b)

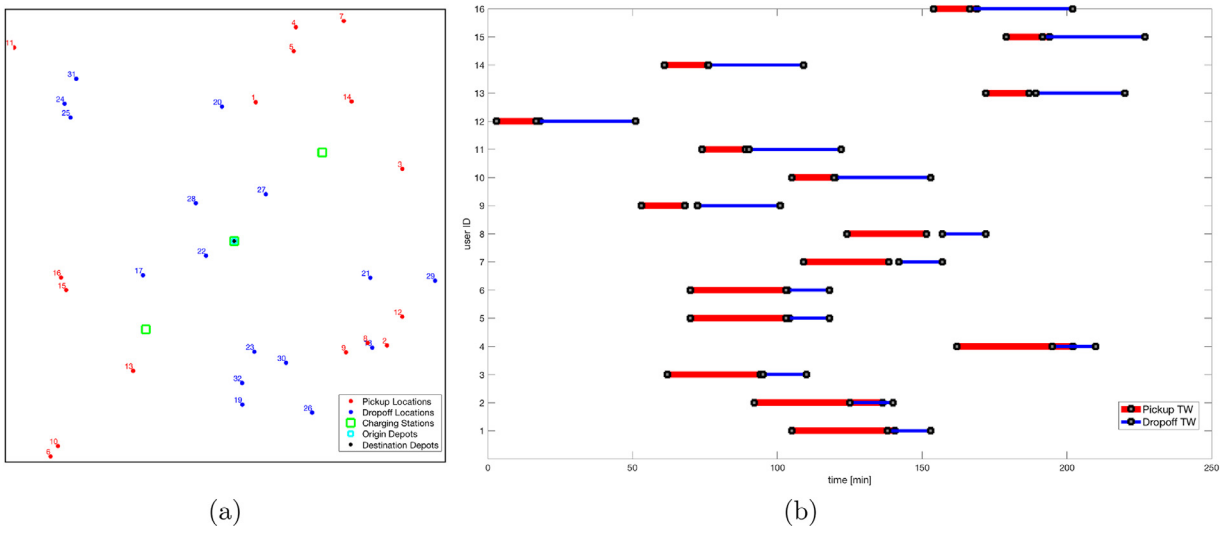

(a) (b)

Fig. 5. Instance a4–16: (a) Pickup and dropoff locations; (b) Pickups and dropoffs time windows after tightening. Note that the pickup location of any user with pickup ID i is denoted by i+16.

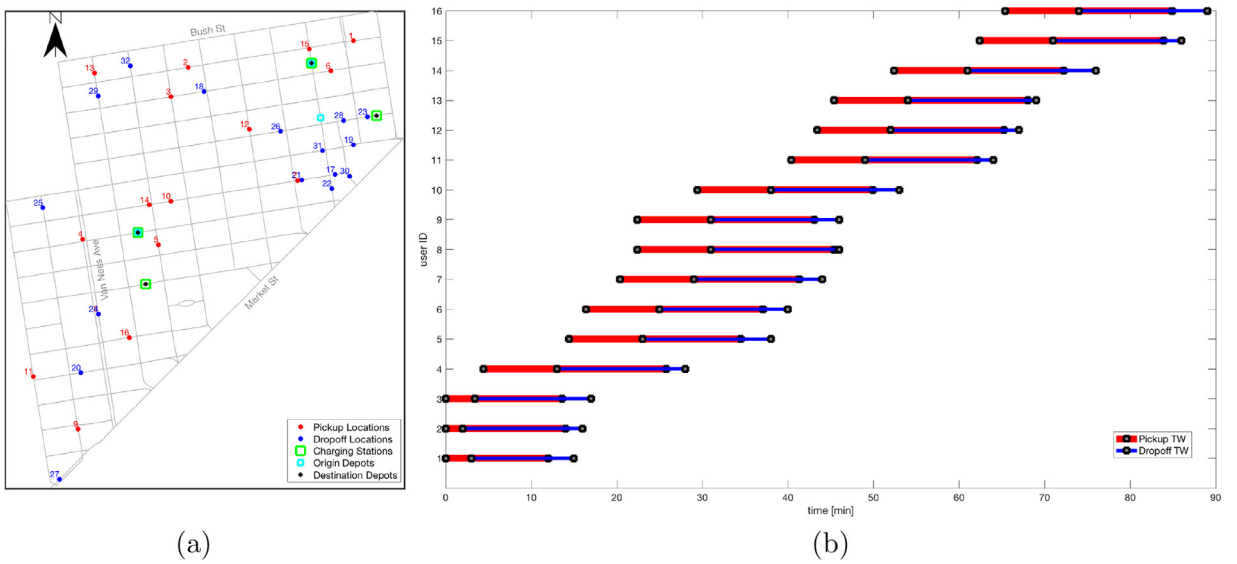

Fig. 6. Instance u4-16: (a) Pickup and dropoff locations; (b) Pickups and dropoffs time windows after tightening. Note that the pickup location of any user with pickup ID i is denoted by i+16.

in Fig. 5(a) can appear anywhere, whereas in Fig. 6(a) they can only appear on the transportation network; (2) after pre-processing, the time windows in Fig. 5(b) are tighter than the time windows in Fig. 6(b); (3) there is more overlap between the pickup and dropoff time windows of the same user in Fig. 6(b) than in Fig. 5(b) (i.e. dropoff time windows are more constraining in the Uber instances); and (4) there is more overlap between the time windows of different users in Fig. 6(b) than in Fig. 5(b) (i.e. users arrival rate is higher for the Uber instances).

In order to scale-up the study region we have focused on, travel times are multiplied by a factor of 2, increase battery consumption by 30%, and reduce the effective battery capacity to 3.5 kWh. Given this transformation, each vehicle can visit at most approximately 15 nodes, with a full effective battery capacity. Again, it is assumed that all vehicles depart from their origin depots with full battery capacities. The maximum ride-times of all users are set to eight minutes and 15 minute time windows are applied at the dropoff locations. In addition, the planning horizon is obtained by considering the dropoff location with the latest service start time and adding the travel time to the furthest charging station. The characteristics of the second set of instances are summarized in Table 2(b). The table follows the same format as Table 2(a).

The objective function weight factors are set to {0.75, 0.25}, i.e. the total vehicle travel time accounts for 75% of the objective function score and the total excess ride-time accounts for 25%. The two datasets used for the computational experiments are available on the website https://luts.epfl.ch/wpcontent/uploads/2019/03/e_ADARP_archive.zip.

5.2. Branch-and-cut results

Next, the performance of the proposed branch-and-cut framework is analyzed for e-ADARP3 and e-ADARP2. In both cases, the default branching strategy of Gurobi is used. In addition, cut generation procedures and separation heuristics are activated at every node in the search tree. Tables 3 and 4 present the computational results obtained for the instances adapted from Cordeau (2006) and Uber respectively, with a time limit of 120 minutes. Note that in the following results, each charging stations may be visited at most once (i.e. the proposed charging-station nodes are not replicated). The first column in Tables 3 and 4 presents the instance name, the second to sixth columns present, for e-ADARP3, the CPU time in minutes, the best solution found, the lower bound, the number of explored nodes, and the number of generated cuts. The seventh to the last columns present the same information for e-ADARP2. Cases where the algorithm is unable to find a feasible solution within the given time limit are denoted by Not Available (NA).

Comparing the computational results of the proposed branch-and-cut algorithm for e-ADARP3 and e-ADARP2 (shown in Tables 3 and 4 respectively), reveals the following observations: (1) e-ADARP2 leads to considerably shorter CPU times with respect to e-ADARP3; (2) in the cases where the optimal solution has not been reached, e-ADARP2 finds stronger lower and upper bounds than e-ADARP3; (3) e-ADARP2 finds a feasible solution to more instances than e-ADARP3; (4) instances with up to 5 vehicles and 40 customers can be solved in Table 3; and (5) instances with up to 4 vehicles and 40 customers can be solved in Table 4.

In order to evaluate the strength of the proposed valid inequalities for the Uber instances, e-ADARP2 is supplemented with each inequality and calculate its performance at the root node. The results of such analysis are reported in Table 5, in which the root node lower bounds are reported as a percentage of the upper bound values. Column LP3 in Table 5 indicates the percentages obtained by solving the LP relaxation of e-ADARP3, whereas column LP2 represents the lower bounds

Table 3
Instances adapted from Cordeau (2006): Comparison between e-ADARP3 and e-ADARP2.

e-ADARP3					e-ADARP2					
Name	CPU	Obj.	LB	Nodes	Cuts	CPU	Obj.	LB	Nodes	Cuts
r=0.1										
a2-16	0.12	237.38*	237.38	170	121	0.02	237.38*	237.38	1	55
a2-20	6.67	279.08*	279.08	10,866	752	0.07	279.08*	279.08	1	108
a2-24	2.58	346.21*	346.21	1768	1106	0.15	346.21*	346.21	132	131
a3-18	7.37	236.82*	236.82	10,339	1466	0.08	236.82*	236.82	1	96
a3-24	21.23	274.81*	274.80	11,022	1874	0.23	274.81*	274.81	299	182
a3-30	120.00	413.27	376.15	27,196	2388	1.70	413.27*	413.27	2362	119
a3-36	120.00	481.72	458.43	20,643	2940	1.78	481.17*	481.17	1561	206
a4-16	52.65	222.49*	222.49	48,594	1826	0.06	222.49*	222.49	126	465
a4-24	120.00	310.84	275.47	22,260	2057	0.52	310.84*	310.84	856	268
a4-32	120.00	413.02	308.14	11,327	3585	10.20	393.96*	393.96	10,389	164
a4-40	120.00	NA	371.71	6463	3658	8.62	453.84*	453.84	5128	386
a4-48	120.00	NA	375.72	2372	4502	120.00	554.54	526.96	36,558	469
a5-40	120.00	490.49	279.56	2024	5242	19.03	414.51*	414.51	10,270	666
a5-50	120.00	NA	359.50	1392	5191	120.00	559.17	531.15	28,368	852
r=0.4										
a2-16	0.13	237.38*	237.38	165	106	0.03	237.38*	237.38	103	135
a2-20	5.97	280.70*	280.70	10,277	730	0.83	280.70*	280.70	1663	89
a2-24	4.20	348.04*	348.04	3644	893	0.42	348.04*	348.04	786	105
a3-18	4.76	236.82*	236.82	5844	1178	0.07	236.82*	236.82	82	92
a3-24	32.89	274.80*	274.80	19,257	1829	0.28	274.81*	274.81	279	186
a3-30	120.00	413.80	369.89	28,757	1986	1.65	413.37*	413.37	2305	96
a3-36	120.00	489.99	452.33	20,961	1741	5.11	484.14*	484.14	3855	204
a4-16	53.20	222.49*	222.49	47,028	1400	0.09	222.49*	222.49	309	529
a4-24	120.00	311.03	281.23	25,986	2467	0.66	311.03*	311.03	1170	278
a4-32	120.00	394.32	307.27	9190	4158	11.36	394.26*	394.26	11,735	156
a4-40	120.00	NA	372.53	5215	712	6.96	453.84*	453.84	3622	430
a4-48	120.00	NA	381.69	3136	4247	120.00	554.60	529.22	38,467	418
a5-40	120.00	454.81	281.44	1639	5811	20.35	414.51*	414.51	12,282	727
a5-50	120.00	NA	372.81	1556	6258	120.00	560.50	528.91	26,189	772
r=0.7										
a2-16	0.49	240.66*	240.66	1223	314	0.09	240.66*	240.66	1360	218
a2-20	120.00	NA	286.06	171,592	529	120.00	NA	287.17	306,306	103
a2-24	58.99	358.21*	358.21	75,993	825	16.02	358.21*	358.21	37,261	123
a3-18	10.71	240.58*	240.58	15,927	1017	0.80	240.58*	240.58	2450	330
a3-24	49.29	277.72*	277.72	29,723	1412	2.54	277.72*	277.72	4265	190
a3-30	120.00	NA	358.79	38,105	2132	120.00	NA	417.06	134,851	98
a3-36	120.00	NA	433.38	20,902	2645	120.00	494.04	485.91	107,714	193
a4-16	36.32	223.13*	223.13	33,176	2246	1.12	223.13*	223.13	5996	690
a4-24	120.00	321.03	279.85	23,100	2435	30.58	318.21*	318.19	73,110	268
a4-32	120.00	NA	302.28	11,142	3083	120.00	430.07	387.99	108,524	131
a4-40	120.00	NA	372.75	5611	389	120.00	NA	443.62	62,465	384
a4-48	120.00	NA	381.98	2107	5281	120.00	NA	524.92	35,901	485
a5-40	120.00	NA	280.02	2264	5817	120.00	447.63	405.99	62,627	582
a5-50	120.00	NA	357.51	1421	7008	120.00	NA	522.37	31,725	751

obtained by solving the LP relaxation of e-ADARP2. The next eight columns present the bounds obtained when supplementing the LP relaxation of the 2-index model with valid inequalities from one of the following families: Generalize Order Constraints (GOC), Subtour Elimination Constraints (SEC), Strengthened Capacity Constraints (SCC), Tournament Constraints (TC), Fork Constraints (FC), Reachability Constraints (RC), Maximum ride-time Constraints (MRT), battery-management Constraints (BM), or Charging Stations Walls Constraints (CSW). Column "Full" reports the bounds obtained when searching for all of the aforementioned families of valid inequalities. The last column presents the upper bound values which are either the optimal values is a solution is found withing the two hour time limit or the best bounds within this time. Note that LP2 includes the separation of capacity, precedence, and pairing constraints. It is therefore possible that LP2 (with no inequalities) presents higher lower bounds than LP2 supplemented with one of the proposed inequalities. Nevertheless, as shown by column "Full", the interaction between all of the proposed inequalities always strengthens the lower bounds at the root node. The results show that, on average over all instances, Maximum Ride-Time (MRT), Reachability (RC) and Subtour Elimination (SEC) constraints have the largest impact on average. However, the relative performance of each inequality is dependent on the minimal battery level ratio, certain inequalities might outperform others. In particular, when the minimal battery level requirement is most restrictive (i.e. $r = 0.7$), Charging Station Walls (CSW) constraints are among the most effective inequalities.

Table 4
Instances from Uber: Comparison between the e-ADARP3 model and the e-ADARP2 model.

e-ADARP3					e-ADARP2					
Name	CPU	Obj.	LB	Nodes	Cuts	CPU	Obj.	LB	Nodes	Cuts
r=0.1										
u2-16	4.47	57.61*	57.61	8058	1025	0.35	57.61*	57.61	1251	1105
u2-20	0.32	55.59*	55.59	372	640	0.16	55.59*	55.59	1	679
u2-24	120.00	91.27	87.52	85,942	1190	7.20	91.27*	91.27	13,482	2081
u3-18	10.50	50.74*	50.74	9286	1251	0.18	50.74*	50.74	357	947
u3-24	120.00	68.78	60.95	32,696	1717	2.17	67.56*	67.56	3819	2450
u3-30	120.00	76.99	70.44	20,711	2021	7.30	76.75*	76.75	7399	4455
u3-36	120.00	109.12	93.01	14,386	2186	18.08	104.04*	104.04	11,540	3556
u4-16	111.94	53.58*	53.58	76,603	1576	0.80	53.58*	53.58	2607	2113
u4-24	57.94	89.83*	89.83	22,915	1607	0.22	89.83*	89.83	251	692
u4-32	120.00	NA	83.93	11,342	2200	19.31	99.29*	99.29	11,686	5093
u4-40	120.00	136.93	111.33	4546	3282	3.09	133.11*	133.11	1915	1093
u4-48	120.00	NA	110.50	2096	3902	120.00	148.30	134.48	19,952	7497
u5-40	120.00	NA	94.21	1831	3624	120.00	121.86	114.12	25,388	8259
u5-50	120.00	NA	114.06	1456	4920	120.00	143.10	132.69	20,580	9141
r=0.4										
u2-16	3.83	57.65*	57.65	7477	1149	0.43	57.65*	57.65	1414	1263
u2-20	1.39	56.34*	56.34	2162	927	0.20	56.34*	56.34	219	445
u2-24	120.00	NA	85.00	85,334	1252	12.62	91.63*	91.63	22,501	1831
u3-18	12.88	50.74*	50.74	14,101	1153	0.23	50.74*	50.74	451	1112
u3-24	120.00	67.77	61.20	34,906	1673	3.68	67.56*	67.56	6589	3051
u3-30	120.00	78.15	70.13	20,729	1756	5.61	76.75*	76.75	5016	4090
u3-36	120.00	NA	93.15	13,127	1902	33.50	104.06*	104.06	19,705	3710
u4-16	88.29	53.58*	53.58	67,819	1341	0.74	53.58*	53.58	2374	2208
u4-24	85.55	89.83*	89.83	37,381	2264	0.47	89.83*	89.83	383	836
u4-32	120.00	NA	84.41	10,821	2399	44.46	99.29*	99.29	29,909	5262
u4-40	120.00	NA	109.74	4001	2909	44.22	133.91*	133.91	31,550	1098
u4-48	120.00	NA	110.43	2125	3833	120.00	NA	133.86	21,713	8262
u5-40	120.00	NA	93.86	1799	4233	120.00	122.23	112.58	27,739	8218
u5-50	120.00	NA	114.00	1475	4683	120.00	143.14	134.09	17,899	9339
r=0.7										
u2-16	25.76	59.19*	59.19	63,296	1117	5.64	59.19*	59.19	19,883	1274
u2-20	2.23	56.86*	56.86	2609	827	1.20	56.86*	56.86	1999	1389
u2-24	120.00	NA	85.98	90,525	1283	120.00	NA	90.83	151,765	1652
u3-18	8.02	50.99*	50.99	7578	1163	0.40	50.99*	50.99	994	1374
u3-24	120.00	69.30	60.36	35,613	1531	6.67	68.39*	68.39	10,163	2080
u3-30	120.00	80.35	69.44	21,115	1783	56.69	78.14*	78.14	58,457	2908
u3-36	120.00	NA	92.30	14,169	1917	120.00	105.79	104.37	73,041	3526
u4-16	120.00	53.87	51.85	52,303	1353	1.48	53.87*	53.87	4872	3304
u4-24	100.76	89.96*	89.96	41,435	1581	0.38	89.96*	89.96	451	656
u4-32	120.00	NA	83.86	9265	2568	47.12	99.50*	99.50	30,099	5173
u4-40	120.00	NA	109.53	4452	2424	120.00	NA	133.01	65,051	826
u4-48	120.00	NA	111.64	1853	3862	120.00	NA	132.49	20,208	7919
u5-40	120.00	NA	94.63	1711	4073	120.00	NA	109.28	29,812	8070
u5-50	120.00	NA	113.94	1426	3546	120.00	144.36	133.33	18,964	9177

5.3. Sensitivity analysis

Multiple charging visits can be modeled by replicating the charging station nodes and imposing symmetry breaking constraints (61). In Table 6 the effect of such replications on the solution quality and performance is analyzed for the Uber instances. The first column of Table 6 displays the instance name. The second to the sixth column report the CPU time (in minutes), objective value, optimality gap, number of visited stations while vehicles are en-route n_{S_R}, and number of visited stations before returning to the depot n_{S_D}, when only a single visit per charging station is allowed. The next five columns present the equivalent information for two allowed visits per charging stations. Finally, the last five columns present the equivalent information for three allowed visits per charging stations. The following observations can be drawn from the results in Table 6: (1) allowing multiple charging visits per station helps in finding a feasible integer solution when no feasible solution could be found with only one visit per station (e.g. instance u4-48 r=0.4); (2) allowing multiple charging visits per station might slightly improve the solution quality, where a maximum objective decrease by 1.72% is experienced by instance u2-16 r=0.7; (3) on average, providing 2 visits per charging station does not significantly increase CPU times, with an average increase by 1.21 min; (4) the increase in CPU time might vary substantially between different instances, with a maximum increase by 63.31 min (instance u3-30 r=0.7) and a maximum decrease by 14.70 min (instance u3-36 r=0.4); (5) two visits per station is the upper bound on the number of charging visits per station for the instances which

Table 5
Instances from Uber: Root node lower bounds as a percentage of the upper bound.

Instance	LP3	LP2	GOC	SEC	SCC	TC	FC	RC	MRT	BM	CSW	Full	U.Bound
r=0.1													
u2-16	81.68	84.87	92.38	89.81	91.40	90.85	88.08	92.91	51.14	86.27	91.05	92.95	57.61
u2-20	94.13	96.24	97.09	73.58	95.85	96.08	96.16	96.01	97.26	96.21	69.49	100.00	55.59
u2-24	72.14	80.64	82.57	82.03	81.29	81.84	60.63	82.84	66.01	55.83	81.10	87.28	91.27
u3-18	85.13	94.12	93.49	93.91	93.59	93.74	94.19	94.07	94.01	93.87	91.12	96.15	50.74
u3-24	78.50	88.05	88.20	88.60	77.78	88.62	88.45	87.84	89.51	88.34	71.62	91.22	67.56
u3-30	80.03	88.22	89.94	90.16	67.38	67.45	88.97	90.29	90.31	89.47	88.55	91.89	76.75
u3-36	80.91	87.44	60.01	65.07	59.97	61.19	66.20	88.46	89.35	88.68	66.78	90.02	104.04
u4-16	73.30	82.07	83.32	83.01	83.10	82.33	82.31	83.18	84.56	83.10	82.13	85.43	53.58
u4-24	76.54	72.82	87.41	88.31	71.98	69.99	73.65	87.10	96.63	87.86	49.32	85.66	89.83
u4-32	76.54	57.12	58.09	81.67	53.35	80.39	76.55	54.97	85.94	58.20	75.24	88.66	99.29
u4-40	74.77	94.49	53.61	76.27	64.85	57.16	54.79	63.63	97.38	74.14	57.68	97.09	133.11
u4-48	64.93	46.80	47.39	48.85	45.08	50.68	51.02	48.40	57.76	44.93	43.87	61.74	148.30
u5-40	69.64	49.01	48.68	48.27	47.23	51.30	49.17	49.98	53.87	48.09	49.10	54.02	121.86
u5-50	69.14	53.38	53.87	54.91	50.51	54.82	57.30	55.43	58.36	53.10	53.97	65.53	143.10
Avg.	76.96	76.80	74.00	76.03	70.24	73.32	73.39	76.79	79.43	74.86	69.36	84.83	
r=0.4													
u2-16	81.75	88.98	90.07	90.97	89.94	90.28	88.98	93.23	92.59	86.87	91.34	93.01	57.65
u2-20	92.11	93.93	95.84	95.65	94.65	95.27	94.86	95.38	93.78	94.65	94.69	97.92	56.34
u2-24	72.05	81.32	81.61	80.35	81.31	81.33	82.19	84.16	84.68	81.26	80.02	86.24	91.63
u3-18	84.91	91.09	93.55	93.59	94.18	93.69	94.12	93.68	94.30	93.67	93.71	94.08	50.74
u3-24	78.31	88.45	88.52	72.37	88.42	89.04	88.49	89.49	89.46	69.74	88.55	90.83	67.56
u3-30	80.19	89.00	90.40	71.72	75.79	89.71	88.79	89.77	88.73	66.56	64.41	91.09	76.75
u3-36	80.95	62.62	56.30	60.87	66.29	67.05	58.95	67.44	69.99	61.59	67.07	80.14	104.06
u4-16	44.69	48.83	41.98	49.27	49.57	48.91	49.37	49.20	50.39	49.57	48.98	51.22	89.83
u4-24	77.86	47.84	88.37	86.93	47.84	86.40	74.02	87.18	96.63	47.84	86.91	94.27	89.83
u4-32	76.40	57.88	75.92	76.61	53.25	58.07	58.87	75.53	77.45	75.61	74.08	88.56	99.29
u4-40	74.12	73.91	72.61	78.02	60.92	74.83	72.20	74.96	95.76	55.45	58.78	97.33	133.91
u4-48	NA	NA	NA	NA	NA	NA	NA	NA	NA	NA	NA	NA	NA
u5-40	70.20	46.95	47.88	50.26	46.82	49.95	47.28	48.03	51.46	48.78	47.78	55.89	122.23
u5-50	69.10	52.54	52.67	54.62	49.26	55.28	55.65	55.28	61.38	53.26	53.71	65.01	143.14
Avg.	75.59	71.03	75.06	73.94	69.10	75.37	73.37	77.18	80.51	68.07	73.08	83.51	
r=0.7													
u2-16	78.41	88.41	49.49	89.75	88.42	88.02	88.41	88.21	90.11	87.38	87.98	90.71	59.19
u2-20	90.11	93.40	94.99	94.60	94.38	94.03	92.77	95.11	93.54	92.75	92.77	96.67	56.86
u2-24	NA	NA	NA	NA	NA	NA	NA	NA	NA	NA	NA	NA	NA
u3-18	84.61	93.01	92.76	93.44	93.09	93.40	92.90	93.45	93.93	93.13	93.30	94.24	50.99
u3-24	77.70	86.94	86.93	88.02	77.92	87.26	88.14	87.73	88.69	87.26	87.10	89.82	68.39
u3-30	77.86	87.62	68.62	88.57	62.35	65.01	88.25	61.76	71.94	64.33	88.32	89.25	78.14
u3-36	79.36	61.96	60.40	64.66	58.27	58.23	59.09	67.70	87.41	59.16	58.11	88.22	105.79
u4-16	74.54	81.98	83.01	83.43	82.16	81.98	82.04	83.02	84.13	82.16	82.60	85.58	53.87
u4-24	76.78	65.67	88.23	86.16	47.77	71.52	71.68	86.75	96.48	47.77	86.78	93.79	89.96
u4-32	76.39	75.60	62.18	83.62	71.98	79.80	84.98	84.28	53.83	53.80	76.93	86.69	99.50
u4-40	NA	NA	NA	NA	NA	NA	NA	NA	NA	NA	NA	NA	NA
u4-48	NA	NA	NA	NA	NA	NA	NA	NA	NA	NA	NA	NA	NA
u5-40	NA	NA	NA	NA	NA	NA	NA	NA	NA	NA	NA	NA	NA
u5-50	69.54	53.87	52.54	53.75	51.77	54.75	55.30	54.98	61.21	52.58	53.94	63.68	144.36
Avg.	78.53	78.85	73.92	82.60	72.81	77.40	80.36	80.30	82.13	72.03	80.78	87.86	

converged to the optimal solution; and (6) providing more than two visits per station might increase the optimality gap when the optimal solution has not been found by the time limit.

Table 7 presents solution details for the Uber instances and provide a comparison when employing internal combustion vehicles. Instances which converge to the optimal solution within the time limit are selected, when two charging visits per station are allowed. Unlike electric vehicles, internal combustion vehicles can operate during the whole planning horizon without the need to refuel. The second to ninth column in Table 7 present results for an electric fleet in which 2 visits per charging station are allowed, as follows: the number of utilized vehicles, the objective function value, the total vehicle travel times (in minutes), the total user excess times (in minutes), the total number of visited charging stations while the vehicles are en-route, the total charging time at the visited charging stations while vehicles are en-route (in minutes), the total number of visited stations before returning to the selected destination depots (i.e. off-route), and the total charging time before returning to the depot (in minutes). The last three columns present the number of utilized vehicles, the objective function value, total vehicle travel time and user excess ride-time when adopting an internal combustion fleet. The following observations can be drawn from the results in Table 7: (1) in some of the proposed instances, vehicles need to recharge en-route and at the end of the planning horizon (e.g. instance u2-24); (2) as expected, en-route recharge can be avoided when the final battery requirements are less restrictive (i.e. r=0.1); (3) vehicles recharge longer when the minimal battery level

Table 6
Instances from Uber: Solution quality and performance when increasing the maximum number of charging visits per station.

	1 visit per station					2 visits per station					3 visits per station				
Name	CPU	Obj.	Gap [%]	n_{S_R}	n_{S_D}	CPU	Obj.	Gap [%]	n_{S_R}	n_{S_D}	CPU	Objective	Gap [%]	n_{S_R}	n_{S_D}
r=0.1															
u2-16	0.35	57.61	0.00	0	1	0.54	57.61	0.00	0	1	2.96	57.61	0.00	0	1
u2-20	0.16	55.59	0.00	0	1	0.11	55.59	0.00	0	1	0.43	55.59	0.00	0	1
u2-24	7.20	91.27	0.00	2	1	14.85	91.27	0.00	2	1	36.05	91.27	0.00	2	1
u3-18	0.18	50.74	0.00	0	0	0.40	50.74	0.00	0	0	0.85	50.74	0.00	0	0
u3-24	2.17	67.56	0.00	0	0	3.94	67.56	0.00	0	0	3.24	67.56	0.00	0	0
u3-30	7.30	76.75	0.00	0	0	5.01	76.75	0.00	0	0	5.24	76.75	0.00	0	0
u3-36	18.08	104.04	0.00	0	3	17.82	104.04	0.00	0	3	18.81	104.04	0.00	0	3
u4-16	0.80	53.58	0.00	0	0	0.92	53.58	0.00	0	0	0.93	53.58	0.00	0	0
u4-24	0.22	89.83	0.00	0	1	0.27	89.83	0.00	0	1	0.32	89.83	0.00	0	1
u4-32	19.31	99.29	0.00	0	0	52.23	99.29	0.00	0	0	52.11	99.29	0.00	0	0
u4-40	3.09	133.11	0.00	0	2	3.70	133.11	0.00	0	2	2.35	133.11	0.00	0	2
u4-48	120.00	148.30	9.32	0	4	120.00	148.37	10.12	0	4	120.00	149.14	9.71	0	4
u5-40	120.00	121.86	6.35	0	1	120.00	121.86	10.14	0	2	120.00	121.86	7.38	0	1
u5-50	120.00	143.10	7.27	0	0	120.00	142.83	5.42	0	1	120.00	142.83	6.96	0	1
r=0.4															
u2-16	0.43	57.65	0.00	0	2	0.86	57.65	0.00	0	2	3.02	57.65	0.00	0	2
u2-20	0.20	56.34	0.00	0	2	0.99	56.34	0.00	0	2	4.31	56.34	0.00	0	2
u2-24	12.62	91.63	0.00	3	1	13.36	91.27	0.00	2	2	54.28	91.27	0.00	2	2
u3-18	0.23	50.74	0.00	0	1	0.38	50.74	0.00	0	1	1.13	50.74	0.00	0	1
u3-24	3.68	67.56	0.00	0	2	2.11	67.56	0.00	0	2	3.63	67.56	0.00	0	2
u3-30	5.61	76.75	0.00	0	2	5.82	76.75	0.00	0	2	3.31	76.75	0.00	0	2
u3-36	33.50	104.06	0.00	0	3	18.80	104.06	0.00	0	3	21.66	104.06	0.00	0	3
u4-16	0.74	53.58	0.00	0	0	1.29	53.58	0.00	0	0	1.91	53.58	0.00	0	0
u4-24	0.74	89.83	0.00	0	2	0.40	89.83	0.00	0	2	0.49	89.83	0.00	0	2
u4-32	44.46	99.29	0.00	0	2	33.86	99.29	0.00	0	2	30.37	99.29	0.00	0	2
u4-40	44.22	133.91	0.00	0	4	104.93	133.68	0.00	1	4	120.00	134.01	0.67	1	4
u4-48	120.00	NA	NA	NA	NA	120.00	150.96	12.00	1	4	120.00	150.78	11.70	1	4
u5-40	120.00	122.23	7.89	0	4	120.00	122.22	8.48	0	4	120.00	121.96	6.27	0	4
u5-50	120.00	143.14	6.32	0	4	120.00	142.83	5.69	0	4	120.00	143.48	8.13	0	4
r=0.7															
u2-16	5.64	59.19	0.00	2	1	2.76	58.17	0.00	1	2	21.91	58.17	0.00	1	2
u2-20	1.20	56.86	0.00	1	2	2.90	56.86	0.00	1	2	14.58	56.86	0.00	1	2
u2-24	120.00	NA	NA	NA	NA	120.00	97.50	7.23	3	2	120.00	NA	NA	NA	NA
u3-18	0.40	50.99	0.00	0	3	0.68	50.99	0.00	0	3	2.54	50.99	0.00	0	3
u3-24	6.67	68.39	0.00	0	3	4.33	68.06	0.00	1	3	8.44	68.06	0.00	1	3
u3-30	56.69	78.14	0.00	1	3	120.00	78.16	0.97	1	3	120.00	78.16	1.31	1	3
u3-36	120.00	105.79	1.34	1	3	120.00	107.65	4.17	1	2	120.00	106.18	2.42	1	3
u4-16	1.48	53.87	0.00	0	3	2.13	53.87	0.00	0	3	2.81	53.87	0.00	0	3
u4-24	0.38	89.96	0.00	1	2	0.49	89.83	0.00	1	2	1.32	89.83	0.00	1	2
u4-32	47.12	99.50	0.00	0	4	33.85	99.50	0.00	0	4	76.03	99.50	0.00	0	4
u4-40	120.00	NA	NA	NA	NA	120.00	137.49	3.16	2	3	120.00	137.61	3.27	2	4
u4-48	120.00	NA	NA	NA	NA	120.00	NA	NA	NA	NA	120.00	NA	NA	NA	NA
u5-40	120.00	NA	NA	NA	NA	120.00	125.14	14.11	0	5	120.00	124.18	10.48	1	5
u5-50	120.00	144.36	7.64	0	5	120.00	164.16	18.84	2	5	120.00	144.10	7.14	1	5

requirement at the selected destination depots is more restrictive (i.e. r=0.7); (4) 3 vehicles out of 4 are utilized to serve the customers in instances u4-16 and u4-24; and (5) utilizing an electric fleet might incur in higher objective function values due to deviations towards charging stations, which may result in either (or both) an increase in the operational cost or a decrease in the quality of service provided to the users.

The e-ADARP extends the standard DARP through several features which have an effect on the total vehicle travel time and user excess ride time. Table 8 analyses the effect derived from two such features, i.e. the choice of the objective function and the use of the electric fleet. The analysis provides results for instances from Cordeau (2006) with up to 5 vehicles and 40 customers. The second to the fourth column report the total vehicle travel time, user excess ride time and optimality gaps for the original e-ADARP2 model, in which up to 1 visit per charging station is allowed. The successive columns present the same results for three relaxed versions of e-ADARP2, i.e. “e-ADARP2 IC fleet”, “e-ADARP2 1 obj.”, and “DARP”. The first omits battery considerations. The second omits excess ride time from the objective function. The third omits both. Note that models “e-ADARP2 1 obj.” and “DARP” provide optimal routing and scheduling solutions which exclusively minimize the total vehicle travel time. Consequently, the scheduling solutions might be sub-optimal in terms of the total user excess ride time. In order to compare the total excess-ride time values provided by all of the proposed models in Table 8, the optimal routing decisions in “e-ADARP2 1 obj.” and “DARP” are fixed and the schedules are post-optimized to minimize the total excess time, as a secondary objective. The post optimization is performed by solving a linear program with the objective

Table 7
Instances from Uber, Electric fleet compared to an internal combustion (IC) fleet: Number of utilized vehicles (Vehs), Total vehicle travel time cost (TT), Users excess ride-time cost (ERT), Total number of visited charging stations en-route (n_{S_R}), Total charging time en-route (E_{S_R}), Total number of visited charging stations off-route (n_{S_D}), Total charging time off-route (E_{S_D}).

	Electric fleet – 2 visits per station								IC fleet			
Name	Vehs	Obj.	TT	ERT	n_{S_R}	E_{S_R}	n_{S_D}	E_{S_D}	Vehs	Obj	TT	ERT
r=0.1												
u2-16	2	57.61	76.81	0.00	0	0.00	1	11.12	2	57.61	76.81	0.00
u2-20	2	55.59	73.70	1.24	0	0.00	1	6.06	2	55.59	73.70	1.24
u2-24	2	91.27	116.98	14.14	2	34.78	1	6.32	2	89.66	114.83	14.14
u3-18	3	50.74	67.65	0.00	0	0.00	0	0.00	3	50.74	67.65	0.00
u3-24	3	67.56	86.08	12.01	0	0.00	0	0.00	3	67.56	86.08	12.01
u3-30	3	76.75	100.83	4.50	0	0.00	0	0.00	3	76.75	100.83	4.50
u3-36	3	104.04	133.79	14.80	0	0.00	3	10.10	3	103.50	131.48	19.57
u4-16	3	53.58	68.76	8.06	0	0.00	0	0.00	3	53.58	68.76	8.06
u4-24	3	89.83	118.21	4.67	0	0.00	1	9.96	3	89.83	118.21	4.67
u4-32	4	99.29	129.19	9.59	0	0.00	0	0.00	4	99.29	129.19	9.59
u4-40	4	133.11	168.40	27.25	0	0.00	2	0.92	4	133.11	168.40	27.25
r=0.4												
u2-16	2	57.65	76.86	0.00	0	0.00	2	23.56	2	57.61	76.81	0.00
u2-20	2	56.34	74.70	1.24	0	0.00	2	39.08	2	55.59	73.70	1.24
u2-24	2	91.27	116.98	14.14	2	34.75	2	56.92	2	89.66	114.83	14.14
u3-18	3	50.74	67.65	0.00	0	0.00	1	11.27	3	50.74	67.65	0.00
u3-24	3	67.56	86.08	12.01	0	0.00	2	34.25	3	67.56	86.08	12.01
u3-30	3	76.75	100.83	4.50	0	0.00	2	50.11	3	76.75	100.83	4.50
u3-36	3	104.06	132.22	19.57	0	0.00	3	86.53	3	103.50	131.48	19.57
u4-16	3	53.58	68.76	8.06	0	0.00	0	0.00	3	53.58	68.76	8.06
u4-24	3	89.83	118.21	4.67	0	0.00	2	25.79	3	89.83	118.21	4.67
u4-32	4	99.29	129.19	9.59	0	0.00	2	123.08	4	99.29	129.19	9.59
u4-40	4	133.68	169.06	27.55	1	1.27	4	59.71	4	133.11	168.40	27.25
r=0.7												
u2-16	2	58.18	76.45	3.36	1	31.69	2	30.12	2	57.61	76.81	0.00
u2-20	2	56.86	75.40	1.24	1	30.50	2	39.08	2	55.59	73.70	1.24
u2-24	2	97.50	125.13	14.62	3	65.28	2	59.21	2	89.66	114.83	14.14
u3-18	3	50.99	67.99	0.00	0	0.00	3	31.11	3	50.74	67.65	0.00
u3-24	3	68.06	85.43	15.96	1	7.03	3	65.86	3	67.56	86.08	12.01
u3-30	3	78.16	102.71	4.50	1	11.75	3	65.09	3	76.75	100.83	4.50
u3-36	3	107.65	136.99	19.63	1	58.93	2	62.46	3	103.50	131.48	19.57
u4-16	3	53.87	69.14	8.06	0	0.00	3	33.91	3	53.59	68.76	8.06
u4-24	3	89.83	118.21	4.67	1	63.71	2	73.32	3	89.83	118.21	4.67
u4-32	4	99.50	128.58	12.26	0	0.00	4	114.20	4	99.29	129.19	9.59

of minimizing the total user excess time and the constraints remaining from the original problem after fixing the routing decisions. The resulting total user excess time is then reported under columns “ERT” for models “e-ADARP2 1 obj.” and “DARP”. Given that the “e-ADARP2 IC fleet” and “DARP” models both assume the use of non-electric vehicles, the results are not affected by changes in the minimum battery level ratio, r.

The following observations are extracted from the results in Table 8: (1) requiring vehicles to return with at least 10% of their battery inventory produces no battery range anxiety; (2) employing an internal combustion fleet saves on average about 2% of the total routing cost, while excess ride time experiences variations by up to 30%; (3) finding feasible solutions to instances $a2-20$, $a3-30$, and $a4-40$ ($r=0.7$) is challenging due to battery considerations; (4) with respect to e-ADARP2, “e-ADARP2 1 obj.” produces solutions in which the total vehicle travel time is only decreased by 2.6%, while the total user excess time is sensibly increased by about 124.45%; and (5) similar to (4), with respect to “e-ADARP2 1 obj.”, “DARP” produces solutions in which the total vehicle travel time is only decreased by 2.48%, while the total user excess ride time is increased by about 117.89%. The results in (4) and (5) demonstrate that considering operational and quality-related criteria in a weighted-sum objective drastically decreases user inconvenience for a moderate increase in transportation cost.

6. Conclusions and future research

In this study, we introduce the electric Autonomous Dial-a-Ride Problem (e-ADARP), which generalizes the standard dial-a-ride problem for the case where electric autonomous vehicles are employed. We present two mixed-integer linear program formulations, namely a 3-index model and a 2-index model. New features incorporated in the problem definition include charging stations, multiple destination depots, partial recharge times, and final battery level requirements. We employ a weighted objective function that accounts for the total travel time of all vehicles and excess ride-time of all users. We develop both new valid inequalities and lifted inequalities from literature by taking into consideration specific properties of

Table 8
Instances from Cordeau (2006): Comparison between the e-ADARP2 model, the e-ADARP2 model when employing an internal combusion fleet, the e-ADARP2 model when only considering total vehicle travel time in the objective function, the standard DARP results (Cordeau, 2006; Ropke et al., 2007; Braekers et al., 2014).

	e-ADARP2			e-ADARP2 IC fleet			e-ADARP2 1obj.			DARP		
Name	TT	ERT	Gap[%]	TT	ERT	Gap[%]	TT	ERT	Gap[%]	TT	ERT	Gap[%]
r=0.1												
a2-16	299.26	51.73	0.00	299.26	51.73	0.00	294.25	72.98	0.00	294.25	73.00	0.00
a2-20	347.89	72.63	0.00	347.89	72.63	0.00	344.83	112.55	0.00	344.83	112.55	0.00
a2-24	433.26	85.08	0.00	433.26	85.08	0.00	413.12	157.41	0.00	413.12	157.41	0.00
a3-18	304.34	34.25	0.00	304.34	34.25	0.00	300.48	119.06	0.00	300.48	119.06	0.00
a3-24	355.78	31.87	0.00	355.78	31.87	0.00	344.83	120.31	0.00	344.83	120.31	0.00
a3-30	500.69	150.99	0.00	500.69	150.99	0.00	494.85	197.18	0.00	494.85	197.18	0.00
a3-36	600.85	122.12	0.00	600.85	122.12	0.00	583.19	244.37	0.00	583.19	244.37	0.00
a4-16	286.45	30.60	0.00	286.45	30.60	0.00	282.68	44.49	0.00	282.68	44.49	0.00
a4-24	388.83	76.88	0.00	388.83	76.88	0.00	375.02	159.65	0.00	375.02	159.65	0.00
a4-32	502.34	68.80	0.00	502.34	68.80	0.00	485.50	165.20	0.00	485.50	165.20	0.00
a4-40	562.44	128.04	0.00	562.44	128.04	0.00	557.69	167.64	0.00	557.69	167.64	0.00
a5-40	524.75	83.78	0.00	524.75	83.78	0.00	498.41	296.37	0.00	498.41	296.37	0.00
r=0.4												
a2-16	299.26	51.73	0.00	299.26	51.73	0.00	294.25	72.98	0.00	294.25	73.00	0.00
a2-20	350.06	72.63	0.00	347.89	72.63	0.00	347.73	112.55	0.00	344.83	112.55	0.00
a2-24	435.70	85.08	0.00	433.26	85.08	0.00	433.46	157.41	0.00	413.12	157.41	0.00
a3-18	304.34	34.25	0.00	304.34	34.25	0.00	300.48	119.06	0.00	300.48	119.06	0.00
a3-24	355.78	31.87	0.00	355.78	31.87	0.00	344.83	120.31	0.00	344.83	120.31	0.00
a3-30	500.83	150.99	0.00	500.69	150.99	0.00	494.84	197.18	0.00	494.85	197.18	0.00
a3-36	615.10	91.29	0.00	600.85	122.12	0.00	588.12	232.74	0.00	583.19	244.37	0.00
a4-16	286.45	30.60	0.00	286.45	30.60	0.00	282.68	44.49	0.00	282.68	44.49	0.00
a4-24	394.48	60.68	0.00	388.83	76.88	0.00	375.02	159.65	0.00	375.02	159.65	0.00
a4-32	502.74	68.80	0.00	502.34	68.80	0.00	485.90	165.20	0.00	485.50	165.20	0.00
a4-40	562.44	128.04	0.00	562.44	128.04	0.00	557.69	167.64	0.00	557.69	167.64	0.00
a5-40	524.75	83.78	0.00	524.75	83.78	0.00	498.41	296.37	0.00	498.41	296.37	0.00
r=0.7												
a2-16	303.64	51.73	0.00	299.26	51.73	0.00	298.63	73.00	0.00	294.25	73.00	0.00
a2-20	NA	NA	NA	347.89	72.63	0.00	NA	NA	NA	344.83	112.55	0.00
a2-24	445.80	95.44	0.00	433.26	85.08	0.00	444.63	194.74	0.00	413.12	157.41	0.00
a3-18	309.36	34.25	0.00	304.34	34.25	0.00	303.71	115.54	0.00	300.48	119.06	0.00
a3-24	359.67	31.87	0.00	355.78	31.87	0.00	350.69	126.34	0.00	344.83	120.31	0.00
a3-30	NA	NA	NA	500.69	150.99	0.00	NA	NA	NA	494.85	197.18	0.00
a3-36	618.01	122.12	1.65	600.85	122.12	0.00	599.75	261.41	0.00	583.19	244.37	0.00
a4-16	282.68	44.49	0.00	286.45	30.60	0.00	282.68	44.49	0.00	282.68	44.49	0.00
a4-24	388.43	107.55	0.00	388.83	76.88	0.00	381.70	149.72	0.00	375.02	159.65	0.00
a4-32	545.17	84.80	9.79	502.34	68.80	0.00	491.23	165.20	0.79	485.50	165.20	0.00
a4-40	NA	NA	NA	562.44	128.04	0.00	NA	NA	NA	557.69	167.64	0.00
a5-40	568.97	83.61	9.30	524.75	83.78	0.00	528.21	283.80	6.97	498.41	296.37	0.00

the e-ADARP. In addition, we design purpose-based separation heuristics to separate the proposed inequalities in a branch-and-cut framework.

Computational experiments are carried out on selected benchmark instances from DARP literature adapted for the e-ADARP, and on a new set of instances based on Uber ride-sharing requests in the city of San Francisco. Results show that, when used in a branch-and-cut framework, the 2-index model outperforms the 3-index model for all of the tested datasets. Based on the root-node analysis, among all of the designed valid inequalities maximum ride-time and reachability constraints are the most effective for the instances derived from Uber ride-shares. Nevertheless, when battery-management aspects are most important, charging station walls constraints are among the most effective inequalities. A sensitivity analysis shows that, for the tested instances, the number of optional visits to charging stations might influence algorithmic performance and solution quality. In particular, CPU times are mostly impacted when the number of optional charging visits per station exceeds the maximum number needed to improve the solution quality. Finally, a sensitivity analysis shows that operating an electric fleet may result in increased operational cost or decreased quality of service (or both) with respect to a traditional internal combustion fleet, due to detours to charging stations.

We design the proposed methodology to solve small-to-medium-sized case scenarios in which all trip requests are booked in advance. Current work is focusing on an efficient metaheuristic approach to solve large-scale instances of the problem proposed in this paper. In addition, the special characteristics of the e-ADARP also generate interesting research directions for the dynamic/on-line case. Specifically, future efforts will focus on the development of on-line algorithms that account for battery-management, detours to charging stations, and incorporation of user excess time as an optimization criterion.

Acknowledgments

This work was supported by the Commission for Technology and Innovation (Innosuisse-Swiss Innovation Agency) [Grant #18045.1 PFES-ES *Innovative fleet management algorithms for planning and operation of autonomous vehicles*]. The authors are grateful to the Innosuisse and the industrial partners from Bestmile who provided insights on the challenges and practices of electric autonomous mini-buses. The authors wish to acknowledge the anonymous reviewers for providing valuable comments on an earlier version of this article. The authors also wish to thank Tim Hillel for proof reading this article.

References

Arslan, O., Yıldız, B., Karaşan, O.E., 2015. Minimum cost path problem for plug-in hybrid electric vehicles. Transp. Res. Part E 80, 123–141.
Ascheuer, N., Fischetti, M., Grötschel, M., 2000. A polyhedral study os the asymmetric traveling salesman problem with time windows. Networks 36, 69–79.
Baldacci, R., Bartolini, E., Mingozzi, A., 2011. An exact algorithm for the pickup and delivery problem with time windows. Oper. Res. 59(2), 414–426.
Baldacci, R., Battarra, M., Vigo, D., 2009. Valid inequalities for the fleet size and mix vehicle routing problem with fixed costs. Networks 54, 178–189.
Baugh, J.W., Kakivaya, G.K., Stone, J.R., 1998. Intractability of the dial-a-ride problem and a multiobjective solution using simulated annealing. Eng. Optim. 30, 2.
Braekers, K., Caris, A., Janssens, G.K., 2014. Exact and meta-heuristics approach for a general heterogeneous dial-a-ride problem with multi depots. Transp. Res. Part B Methodol. 67, 166–186.
Braekers, K., Kovacs, A.A., 2016. A multi-period dial-a-ride problem with driver consistency. Transp. Res. Part B Methodol. 94, 355–377.
Cordeau, J.-F., 2006. A branch-and-cut algorithm for the dial-a-ride problem. Oper. Res. 54 (3), 573–586.
Cordeau, J.-F., Laporte, G., 2003. A tabu search heuristic for the static multi-vehicle dial-a-ride problem. Transp. Res. Part B Methodol. 37 (6), 579–594.
Desaulniers, G., Errico, F., Irnich, S., Schneider, M., 2016. Exact algorithms for electric vehicle-routing problems with time windows. Oper. Res. 64(6), 1388–1405.
Doppstadt, C., Koberstein, A., Vigo, D., 2016. The hybrid electric vehicle-traveling salesman problem. Eur. J. Oper. Res. 253. 852–842
Dunning, I., Huchette, J., Lubin, M., 2017. Jump: a modeling language for mathematical optimization. SIAM Rev. 59 (2), 295–320.
Erdoğan, S., Miller-Hooks, E., 2012. A green vehicle routing problem. Transp. Res. Part E Logist. Transp. Rev. 48(1), 100–114.
Felipe, Á., Ortuño, M., Righini, G., Tirado, G., 2014. A heuristic approach for the green vehicle routing problem with multiple technologies and partial recharges. Transp. Res. Part E 71, 111–128.
Genikomasakis, K., Mitrentsis, G., 2017. A computationally efficient simulation model for estimating energy consumption of electric vehicles in the context of route planning applications. Transp. Res. Part D Transp. Environ. 50, 98–118.
Goeke, D., Schneider, M., 2015. Routing a mixed fleet of electric and conventional vehicles. Eur. J. Oper. Res. 245, 81–99.
Gschwind, T., Inrich, S., 2014. Effective handling of dynamic time windows and its application to solving the dial-a-ride problem. Transp. Sci. 49(2), 335–354.
Healy, P., Moll, R., 1995. A new extension of local search applied to the dial-a-ride problem. Eur. J. Operat. Res. 83 (1), 83–104.
Hiermann, G., Puchinger, J., Ropke, S., Hartl, R., 2016. The electric fleet size and mix vehicle routing problem with time windows and recharging stations. Eur. J. Oper. Res. 252, 995–1018.
Keskin, M., Çatay, B., 2016. Partial recharge strategies for the electric vehicle routing problem with time windows. Transp. Res. Part C Emerg. Technol. 65, 111–127.
Lu, Q., Dessouky, M.M., 2004. An exact algorithm for the multiple vehicle pickup and delivery problem. Transp. Sci. 38(4), 503–514.
Lysgaard, J., 2006. Reachability cuts for the vehicle routing problem with time windows. Eur. J. Oper. Res. 175, 210–223.
Masmoudi, M.A., Hosny, M., Demir, E., Genikomsakis, K.N., 2018. The dial-a-ride problem with electric vehicles and battery swapping stations. Transp. Res. Part E Log. Transp. Rev. 118, 392–420.
Molenbruch, Y., Braekers, K., Caris, A., 2017. Typology and literature review for dial-a-ride problems. Ann. Oper. Res. 259 (1–2), 295–325.
Molenbruch, Y., Braekers, K., Caris, A., Berghe, G.V., 2017. Multi-directional local search for a bi-objective dial-a-ride problem in patient transportation. Comput. Operat. Res. 77, 58–71.
Parragh, S.N., 2011. Introducing heterogeneous users and vehicles into models and algorithms for the dial-a-ride problem. Transp. Res. Part C Emerg. Technol. 19(5), 912–930.
Parragh, S.N., Doerner, K.F., Hartl, R.F., Gandibleux, X., 2009. A heuristic two-phase solution approach for the multi-objective dial-a-ride problem. Networks 54(4), 227–242.
Parragh, S.N., Schmid, V., 2013. Hybrid column generation and large neighborhood search for the dial-a-ride problem. Comput. Operat. Res. 40(1), 490–497.
Pelletier, S., Jabali, O., Laporte, G., 2016. 50Th anniversary invited article - goods distribution with electric vehicles: review and research perspectives. Transp. Sci. 50(1), 3–22.
Pelletier, S., Jabali, O., Laporte, G., 2018. Charge scheduling for electric freight vehicles. Transp. Res. Part B Methodol. 115, 246–269.
Pelletier, S., Jabali, O., Laporte, G., Veneroni, M., 2017. Battery degradation and behavior for electric vehicles: review and numerical analyses of several models. Transp. Res. Part B Methodol. 103, 158–187.
Raviv, T., Kaspi, M., 2012. The locomotive fleet fueling problem. Oper. Res. Lett. 40, 39–45.
Ropke, S., Cordeau, J.-F., 2009. Branch and cut and price for the pickup and delivery problem with time windows. Transp. Sci. 43 (3), 267–286.
Ropke, S., Cordeau, J.-F., Laporte, G., 2007. Models and branch-and-cut algorithms for pickup and delivery problems with time windows. Networks 49 (4), 258–272.
Ruland, K.S., Rodin, E.Y., 1997. The pickup and delivery problem: faces and branch-and-cut algorithm. Comput. Math. Appl. 33(12), 1–13.
Savelsbergh, M.W., 1985. Local search in routing problems with time windows. Ann. Oper. Res. 4 (1985/6), 285–305.
Schiffer, M., Walther, G., 2017. The electric location routing problem with time windows and partial recharging. Eur. J. Oper. Res. 260(3), 995–1013.
Schneider, M., Stenger, A., Goeke, D., 2014. The electric vehicle-routing problem with time windows and recharging stations. Transp. Sci. 48(4), 500–520.
Toth, P., Vigo, D., 2014. Vehicle Routing Problems, Methods, and Applications, (Second ed.) SIAM, Philadelphia Monograph on Discrete Mathematics and Applications.